

HISTORIC AMERICAN ENGINEERING RECORD
BOSTON & MAINE RAILROAD, BERLIN BRANCH BRIDGE #148.81
(Moose Brook Bridge)
HAER No. NH-48

Location: Originally located on the Boston & Maine Railroad crossing of the Moose Brook on the north side of US 2, .75 miles west of NH 16, Gorham, Coos County, New Hampshire. The bridge was located at 44.40049, -71.20759 until it burned in 2004. It was reconstructed and moved to Case Western Reserve University in Cleveland, Ohio for research from 2011-2014, temporarily located at: 41.502540, -81.606353. In 2017-2018 it was moved, reassembled, and permanently placed over Trout Brook on the excursion line of the Wiscasset, Waterville and Farmington Railway Museum in Alna, Lincoln County, Maine, located at 44.099291, -69.622936. The coordinates were obtained in December 2018 in Google Earth.

Structural Type: Howe boxed pony truss

Construction Dates: Built 1918; burned 2004; reconstructed 2011-2012; final assembly 2017-18

Builder: Boston & Maine Railroad

Present Owner: The National Society for the Preservation of Covered Bridges transferred ownership to the Wiscasset, Waterville and Farmington Railway Museum on June 9, 2018

Present Use: Railroad bridge on excursion rail line

Significance: The Moose Brook Bridge is one of six boxed pony truss bridges remaining in North America. This former rail line contributed to the economic development of Coos County and the growth of tourism in the White Mountains.

Authors: Lola Bennett (history), 2009; Dario Gasparini and Kamil Nizamiev (engineering), 2018; Timothy Andrews (reconstruction); Vern Mesler (brazing); Christopher H. Marston (editor), 2019

Project Information: The National Covered Bridges Recording Project is part of the Historic American Engineering Record (HAER), a long-range program to document historically significant engineering and industrial works in the United States. HAER is administered by the Heritage Documentation Programs division of the National Park Service, U.S. Department of the Interior. The Federal Highway Administration's National Historic Covered Bridge Preservation Program (Sheila Rimal Duwadi, administrator) funded the project.

Christopher H. Marston, HAER Architect, served as project leader from 2009-2019. The 2009 HAER field team consisted of Anne E. Kidd, field supervisor; Jeremy T. Mauro and Bradley M. Rowley, architects; and Csaba Bartha, ICOMOS intern (Romania); Lola Bennett, historian; and Jet Lowe, photographer. The National Society for the Preservation of Covered Bridges (NSPCB, David Wright, president until he died in 2014) offered the bridge for the research project. Timothy Andrews of Barns and Bridges of New England (BBofNE) disassembled the bridge in 2010, and reconstructed the trusses in 2011-2012, assisted by Will Truax. Vern Mesler led the braze welding repair of the castings at Lansing Community College in 2011. Dario Gasparini led the engineering research on the trusses at Case Western Reserve University, from 2011-2014, assisted by staff Kamil Nizamiev, Neil Harner, Jim Berilla, Michael Butler, and David Conger; and students Vincent Marvin, Lin Wan, and Janette Siu. In 2013, HAER completed laser scanning of the trusses, with a field team consisting of Jeremy T. Mauro, field supervisor, Pavel Gorokhov, Ben Shakelton, and Hummam Salih, architects. Under a Phase II agreement with the NSPCB (William Caswell, president since 2014), Timothy Andrews reassembled the trusses at the Wiscasset, Waterville and Farmington Railway Museum (WW&F; David J. Buczkowski, president) in 2017-2018.

CHRONOLOGY

- 1803 Coos County, New Hampshire, formed
- 1805 America's first covered bridge erected at Philadelphia
- 1830 ca. America's first covered railroad bridge erected for Baltimore & Ohio Railroad
- 1835 Boston & Maine Railroad (B&M) chartered by the Massachusetts Legislature
- 1840 William Howe (1803-1852) patents Howe truss
- 1844 Boston, Concord & Montreal Railroad (BC&M) chartered
- 1848 White Mountains Railroad chartered
- 1889 BC&M merges with Concord Railroad to form the Concord & Montreal Railroad
- 1891 Concord & Montreal RR begins construction of line from Whitefield to Berlin, New Hampshire
- 1893 Concord & Montreal RR completes line from Whitefield to Berlin
- 1895 B&M leases Concord & Montreal Railroad for ninety-one years
- 1917 B&M begins upgrading structures on Berlin Branch
- 1918 Moose Brook Bridge completed at milepost 148
- 1983 Guilford Transportation acquires Boston & Maine Railroad
- 1989 New Hampshire & Vermont Railroad acquires B&M Berlin Branch
- 1996 New Hampshire & Vermont Railroad abandons B&M Berlin Branch
- 1997 Railroad tracks removed between Jefferson and Berlin
- 1999 State of New Hampshire develops Presidential Range Rail Trail on former Berlin Branch
- 2004 Moose Brook Bridge burns; NSPCB salvages trusses for potential reuse
- 2009 HAER records Moose Brook Bridge; Case Western Reserve University funded by Federal Highways Administration for a Howe truss study and drafts agreement with NSPCB for use of trusses
- 2010 Timothy Andrews disassembles trusses and moves salvage members to Campton, New Hampshire
- 2011 First truss is reconstructed at Campton and shipped to Cleveland in August; Vern Mesler completes brazing repair of cracked castings in the fall
- 2012 Second truss is reconstructed and shipped to Cleveland; both trusses post-tensioned and installed beneath prestressed cover at Case Western Reserve University for research
- 2014 Trusses are disassembled and shipped from Cleveland back to Gorham, New Hampshire
- 2017 NSPCB reaches an agreement with Wiscasset, Waterville and Farmington Railway Museum to reuse the bridge; Howe trusses are shipped to Alna, Maine
- 2018 Final reassembly of Moose Brook Bridge completed. Ownership transferred from NSPCB to WW&F on June 9. In September, the bridge is erected over Trout Brook as part of an extension of the WW&F excursion line

DESCRIPTION

Moose Brook Bridge is a single-span wood and iron Howe pony truss bridge.¹ The structure has an overall height of 11'-1", 19'-6" width (18'-0" center to center of trusses), and 46'-10" length (end to end). Prior to being seriously damaged in a 2004 arson fire, the bridge spanned Moose Brook on 20' high stone masonry abutments; the east abutment was replaced with concrete at an unknown date. From 2004-2010, the charred trusses rested on land adjacent to the northeast corner of a replacement bridge. The span's vertical plank siding, portions of braces and outriggers, and much of the deck were destroyed in the blaze. The following is a detailed description of the original structure prior to the fire, with supplemental information from Timothy Andrews.

Each truss has six panels. The top chords are paired 10" x 12" timbers, the bottom chords are paired 10" x 16" timbers. The pairs of chord sticks are bolted together with 3" spacer blocks. The top and bottom chords are connected by vertical tension rods, paired diagonal braces and single counterbraces, and end posts. The size of the vertical tension rods increases in diameter from the center to the ends of the spans. The center rod is 2-³/₄" diameter with 3" upset threads and a 5" nut; the interior panel rods are 3" diameter with 3-¹/₄" upset threads and 5" nuts; the end rod is 3-¹/₂" diameter with 4" upset threads and 6" nuts. The diagonals increase in section from 8" x 8" at the center panel to 8" x 10" at the intermediate to 10" x 12" at the end panel. The counterbraces decrease in size from 6" x 7" at the center panel, to 4" x 8", and then 3" x 7" at the end panel. There are two sets of paired 4" x 10" end posts at each end, with paired 1" diameter vertical rods in between. The diagonal braces are seated on triangular-shaped cast-iron metal shoes, notched into the top and bottom chords. There are seven castings on the bottom chord and five on the top chord. Instead of a casting at the top of each end panel there is a 7" x 1'-1-¹/₂" wood thrust block to receive the counterbrace and the inner end posts. The vertical rods pass through the metal shoes and between the top and bottom chord members. The rods are fastened to the chords with a 1'-6" square plate washer, a 1'-2" square plate, and a 5-³/₄" washer; the plate washers are proportionately larger for the 3-¹/₂" rods.

The floor system is composed of 10" x 16" transverse floor beams that hang below the bottom chord, three floor beams per bay, spaced approximately 24" apart. There were originally four lines of 7-³/₈" x 9-³/₄" stringers laid longitudinally on top of the floor beams and 6" x 8" x 9" railroad ties laid transversely on top of the stringers. The 4'-8-¹/₂" standard gauge iron rails were fastened longitudinally on the ties. The rails and ties were removed in 1997 and replaced with a wood deck.

¹ Although formally named the Berlin Branch Bridge #148.81, the structure is referred to in this report as the Moose Brook Bridge for simplicity.

There are lateral tie rods consisting of 1-1/4" diameter rods with turnbuckles between the bottom chords at each portal. Sway bracing consists of two 12" x 16" timber outriggers that span the full width of the bridge and extend 6'-6" beyond the outer faces of the bottom chords with 1" iron tension rods fastened from the top chord to the outer end of the outriggers. The boxed pony trusses are sheathed with 1" x 6" vertical plank siding, angled at the top to allow rainwater to drain. Originally there were four 2'-6" square plywood access panels located at each panel point along the inside of the trusses, the same as found on its sister bridge, the Snyder Brook Bridge.²

DESIGN

During the 1830s and 1840s, demand increased for standardized bridges that could be rapidly erected and easily maintained to keep pace with the growth of the nation's railroad network. In 1838, Massachusetts millwright William Howe (1803-1852) built the first Howe truss bridge for the Western Railroad at Warren, Massachusetts.³ Howe's timber truss design had parallel top and bottom chords connected by wood diagonals (compression members) and iron verticals (tension members). First to incorporate iron for primary structural members, the Howe truss improved on the 1830 Long truss by replacing the vertical posts with adjustable wrought-iron rods to overcome the inherent difficulty of creating tension connections in wood structures and allowing for easier and more efficient prestressing of the members. In 1840, Howe received a patent for his truss design.

Howe sold patent rights to companies nationwide, and the Howe truss soon became the most widely used wood truss for railroad bridges. Railroads favored the Howe truss design because it could be erected quickly and adjusted easily. An article in the 1878 *Transactions of the American Society of Civil Engineers* stated, "the Howe truss may justly be termed the most perfect wooden bridge ever built; others have been designed of greater theoretical economy; but for simplicity of construction, rapidity of erection, and general utility it stands without rival."⁴

Used extensively for railroad bridges in the United States and Europe during the mid-nineteenth century, the timber Howe truss gradually gave way to similar structures with cast-iron compression members and wrought-iron tension members.⁵ There are well over 100 timber

² Timothy Andrews email to Christopher Marston, November 30, 2011. See: Historic American Engineering Record (HAER), National Park Service, U.S. Department of the Interior, "Boston & Maine Railroad, Berlin Branch Bridge #143.06 (Snyder Brook Bridge)," HAER NY-49.

³ Richard Sanders Allen, *Covered Bridges of the Northeast* (Brattleboro, VT: Stephen Greene Press, 1957), 18. The Quaboag River Bridge was replaced in 1873 with a larger Howe truss covered bridge capable of carrying double tracks.

⁴ "Bridge Superstructure," *Transactions of the American Society of Civil Engineers* (1878), 340.

⁵ There are two surviving all-iron Howe pony trusses from 1845-46 built by the Reading Railroad, one on private property and one moved to the Smithsonian. See: Richard K. Anderson and Emory L. Kemp, "Reading-Halls

Howe truss covered bridges surviving in the United States, although as of 2019, fewer than six surviving were originally built to carry railroads.⁶

BOXED PONY TRUSS BRIDGES

While not as picturesque as traditional covered bridges, boxed pony trusses are a product of the same era and building traditions. Low trusses, or “pony” trusses, are an economical way to build short-span bridges. Because of their height, pony truss bridges do not have overhead bracing and, when built of wood, need to be housed differently than full-height timber bridges to allow for the passage of vehicles. The most common solution was to cover each truss separately, leaving the deck uncovered. No one knows how many wooden pony truss bridges once existed, but as of 2009, there were only eight known historic survivors in North America. As of 2019, a total of six remain; two have been reconstructed.

WORLD GUIDE #	HAER #	BRIDGE	COUNTY	ST	DATE	TYPE	BUILDER
07-04-P1x		COMSTOCK	MIDDLESEX	CT	1873	HOWE	UNKNOWN
07-04-P1#2		COMSTOCK	MIDDLESEX	CT	2011	HOWE	MCFARLAND JOHNSON
29-04-P1x	NH-48	MOOSE BROOK	COOS	NH	1918	HOWE	B&M RR
19-08-P6	NH-48	TROUT BROOK	LINCOLN	ME	2018	HOWE	B&M RR
29-04-P2	NH-49	SNYDER BROOK	COOS	NH	1918	HOWE	B&M RR
29-06-P1	NH-43	LIVERMORE	HILLSBOROUGH	NH	1937	TOWN	UNKNOWN
29-09-P1	NH-44	ROLLINS FARM	STRAFFORD	NH	1929	HOWE	B&M RR
38-09-P1	PA-623	MEAN’S FORD/ BURNT MILL	BUCKS	PA	ca.1860	HOWE	UNKNOWN
61-02-P1		PONT BLANC	ABITIBI-QUEST	QU	ca.1947	TOWN	DEPT. COLONIZATION
61-02-P11x		PONT DE LA TRAVERSE	ABITIBI-QUEST	QU	ca.1949	TOWN	DEPT. COLONIZATION

Notes: Several changes have occurred to these structures since the list was first compiled in 2009 (lost bridges in gray). Comstock Bridge was reconstructed in 2011. Snyder Brook Bridge was rehabilitated in 2015. Pont de la Traverse was lost to a flood in 2012. Pont Blanc remains a ruin as of 2019. As

Station Bridge,” HAER No. PA-55, Historic American Engineering Record (HAER), National Park Service, U.S. Department of the Interior, 1987.

⁶ Clark’s Bridge (ca. 1904), a well-preserved Howe truss that is the only covered bridge carrying active rail traffic in the United States as part of the short excursion line at Clark’s Trading Post in Lincoln, New Hampshire. See: Historic American Engineering Record (HAER), National Park Service, U.S. Department of the Interior, “Clark’s Bridge,” HAER NH-39. The reconstructed Moose Brook Bridge erected over Trout Run for WW&F will become the second active covered railroad bridge in 2020.

described here, the Moose Brook Bridge burned in 2004, was reconstructed in 2011-12, and erected over Trout Brook for the Wiscasset, Waterville and Farmington Railway Museum in Maine in 2018.

HISTORY

From 1891-1893, the Concord & Montreal Railroad built a 30-mile, single-track branch line from its main line at Whitefield, New Hampshire, to Berlin, where lumber and paper industries were booming.⁷ The line passed through the towns of Jefferson, Randolph, and Gorham, along the northern edge of the Presidential Range. Shortly after the line’s completion, the Boston & Maine Railroad leased the branch for ninety-one years.

No information has been found concerning the first bridge at this location, but presumably it was a wood structure. World War I brought the need for longer, heavier, and faster freight loads on this division, and much of the line was upgraded to accommodate heavier rolling stock. At least three Howe pony truss bridges were built on the line in 1918.⁸

C&M RR #	B&M RR #	TOWN	CROSSING	TYPE	SPAN	NOTES
254	143.06	RANDOLPH	SNYDER BROOK	HOWE PONY TRUSS	28'-9"	REHABBED 2015
255	144.13	RANDOLPH	BUMPUS BROOK	HOWE PONY TRUSS	27'-4"	BURNED 1964
262	148.81	GORHAM	MOOSE BROOK	HOWE PONY TRUSS	39'-6"	BURNED 2004 MOVED 2018

The line saw regular use for both passenger and freight trains until the 1960s. The line was leased to Guilford in 1983 and to New Hampshire & Vermont Railroad in 1989. In 1996, the corridor from Waumbek Junction to Berlin was abandoned, and the New Hampshire Division of Parks and Recreation (Department of Resources and Economic Development) purchased and converted it for a multiple-use recreational trail.⁹

In May 2004, vandals set fire to the Moose Brook Bridge. Afterwards, New Hampshire State Architectural Historian James Garvin contacted the National Society for the Preservation of Covered Bridges for assistance in preserving the structure. The NSPCB, then under the leadership of David Wright, subsequently took ownership of the bridge from the New Hampshire Department of Transportation (NHDOT), and hired Timothy Andrews of Barns and Bridges of

⁷ Concord & Montreal Railroad, *Second Annual Report of the Directors*, June 30, 1891 (Concord: New Hampshire Democratic Press Co., 1891), 14.

⁸ It is possible that there were other pony truss bridges on this line, but records haven;t been found for the entire line.

⁹ “New Hampshire’s Presidential Rail Trail,” <https://www.railstotrails.org/trailblog/2014/december/09/new-hampshire-s-presidential-range-rail-trail/>, last updated December 9, 2014. The section of track from Whitefield to Waumbek Junction is still used by the New Hampshire Central Railroad.

New England (BBofNE) to remove the charred trusses from the abutments.¹⁰ A wooden replacement bridge was constructed for continued rail-trail use. From 2004-2010, the trusses sat alongside the trail, several yards from the northeast corner of the new bridge.

BUILDER

Some of the earliest railroad bridges were timber structures because wood was abundant, cheap, and easy to work with. Lewis Wernwag built the first wood railroad bridge in the United States for the Baltimore & Ohio Railroad over the Monocacy River in Maryland ca. 1830.¹¹ Within a short time, wooden truss bridges were commonplace on America's growing network of railroads. Thousands of timber railroad bridges (both covered and uncovered) were built in the nineteenth century. In 1841, one English traveler noted: "The timber bridges of America are justly celebrated for their magnitude and strength. By their means the railways of America have spread widely and extended rapidly."¹²

By the late nineteenth century, most railroad bridges were being built of iron or steel. The Boston & Maine Railroad was an exception. The company continued to build timber bridges into the early twentieth century. This was largely due to the efforts of Jonathan Parker Snow (1848-1933), an advocate of timber bridges, who served as an engineer for the Boston & Maine Railroad from 1888 to 1911.¹³

Early in his railroad work, J. P. Snow became convinced that wooden truss bridges should be maintained in service for as long as possible instead of being replaced with iron trusses. In 1895, nearly 70 percent of the bridges on the Boston & Maine Railroad were wood. It was accepted that wooden bridges might have a shorter service life, but they could be easily reinforced if necessary and they gave ample evidence of distress long before failure. Snow advocated use of the Town lattice truss for long spans and the Howe truss for spans of 30' to 60'.¹⁴ By the 1930s, the increased weight of rolling stock had led to the replacement of most wooden railroad bridges with metal truss bridges.¹⁵

¹⁰ James L. Garvin, "Chronology of Planning and Work: Boxed Railroad Pony Truss Bridge, Gorham, New Hampshire," unpublished manuscript, 2009.

¹¹ Theodore Cooper, "American Railroad Bridges," *Transactions of the American Society of Civil Engineers* 21 (July 1889): 10; Richard Sanders Allen, *Covered Bridges of the Middle Atlantic States* (Brattleboro, VT: Stephen Greene Press, 1959), 18-19.

¹² Allen, *Covered Bridges of the Northeast*, 94.

¹³ See Joseph D. Conwill, "Wright's Bridge," HAER No. NH-35, Historic American Engineering Record (HAER), National Park Service, U.S. Department of the Interior, 2002.

¹⁴ J.P. Snow, "Wooden Bridge Construction on the Boston & Maine Railroad," *Journal of the Association of Engineering Societies* (July 1895), 35.

¹⁵ Robert Fletcher and J.P. Snow, "A History of the Development of Wooden Bridges," *Proceedings of the American Society of Civil Engineers* (November 1932).

APPENDIX: ENGINEERING REPORT

AUTHORS: Dario Gasparini and Kamil Nizamiev, 2018

INTRODUCTION

The Howe truss is one of the most significant structural forms devised in the United States in the nineteenth century. Its simplicity perfectly suited two transformative technological and cultural changes that occurred in American construction practice in the nineteenth century: the industrialization of fabrication and the rationalization of structural design based on developments in engineering science. A Howe truss used significant amounts of iron; the production of large castings and threaded wrought-iron rods required shop-based fabrication. Moreover, since the Howe truss featured simple square-ended wood members, wood fabrication could also be done in a shop, and on-site erection did not require expert heavy timber framers. The industrialization of Howe bridge fabrication stimulated the formation of several bridge companies beginning in the 1840s.

Until the late 1820s, bridges were realized largely based on empirical knowledge and experience acquired and controlled by master builders such as Timothy Palmer, Theodore Burr, and Lewis Wernwag. Beginning in the 1830s, the American engineer Col. Stephen H. Long began designing truss bridges using equilibrium-based structural analyses, motivated by the needs of the emerging railroads and based largely on developments in engineering science by Claude-Louis Navier. Long was the first U.S. engineer to calculate the loads that a bridge could safely carry. He designed the Jackson Bridge in 1830 for the Baltimore and Ohio Railroad (B&O) to carry two railroad tracks, which he estimated produced an effective distributed load of 120 pounds (lbs) per square foot of floor area.¹⁶ Engineering science-based design and shop prefabrication effectively shifted control of bridge construction away from master builders toward engineers.

The Howe truss, patented by millwright William Howe, was first implemented on a large scale through engineering design by Colonel Long's protégé, George Washington Whistler. An 1819 graduate of West Point, Whistler was appointed chief engineer for the Western Railroad of the State of Massachusetts in 1839. The first large-scale use of the Howe truss form was for the Western Railroad's bridge over the Connecticut River, completed in July 1841.¹⁷ Contemporary

¹⁶ Justine Christianson and Christopher H. Marston, executive editors, *Covered Bridges and the Birth of American Engineering* (Washington, DC: Historic American Engineering Record, National Park Service 2015), 130-135.

¹⁷ D. A. Gasparini, "Whistler, Howe, and Stone: The Design and Construction of the Western Railroad's Bridge over the Connecticut River 1840-1841," *Proceedings of the Fifth International Congress on Construction History*, Chicago, IL (June 3-7, 2015), 161-168.

engineering literature praised the completion of the bridge, and it became a transformative event in the history of American railroad bridge design and construction. The Western Railroad adopted the Howe form for all its truss bridges from Springfield, Massachusetts, to Albany, New York. It subsequently became the dominant bridge type for the rapidly growing U.S. railroads for over thirty years, until the transition to more durable all-iron bridges in the 1860s and 1870s. It is effectively impossible to estimate the number of Howe bridges built by U.S. railroads in the nineteenth century because ever increasing railway loads and the national adoption of the form by numerous railroad companies resulted in the rapid replacement of railroad bridges. Miller provides quantitative evidence on the dominance of the Howe truss in just the state of Ohio. He examined the *Annual Reports of the Commissioners of Railroads and Telegraphs in Ohio* for the years 1882 through 1884. Inspection data given in the reports revealed that about 1,000 covered and uncovered wooden truss railroad bridges existed in Ohio in the 1880s, most built from 1868 to 1875. The data indicated that approximately 95 percent of all the wooden truss railroad bridges used Howe trusses.¹⁸

Largely because of engineers G. W. Whistler and Carl Ghega, Howe truss technology quickly spread to Europe and Russia.¹⁹ Howe truss bridges abound in Switzerland, Austria, and southern Germany. The extant 1852 King Ludwig Bridge in Kempten, Germany, is perhaps the finest extant example of the earliest Howe truss design, which used wood bearings for diagonals that spanned over two panels.²⁰

The Howe truss also had a major impact on long-span roof and floor construction, although this history is not well-documented. The Howe truss was used often in an arc form for long-span roofs of railroad stations, such as the 1850 President Street Station in Baltimore, Maryland.²¹ The Howe roof truss was also used for warehouses and early locomotive roundhouses, as shown in Figure 1. A later example found at the Cleveland Elysium, completed in 1907, can be seen in Figure 2.

¹⁸ Terry Miller, "Ohio Rail Covered Bridges," unpublished manuscript, 1967.

¹⁹ D. A. Gasparini, K. Nizamiev, and C. Tardini, "G.W. Whistler and the Howe Bridges on the Nikolaev Railway, 1842-1851," *ASCE Journal of Performance of Constructed Facilities* 30, no. 3 (June 2016): 1-16.

²⁰ Stefan M. Holzer, *Die König-Ludwig-Brücke Kempten*, Historische Wahrzeichen Ingenieurbaupunkunst in Deutschland, Band 11 (Berlin: Bundesingenieurkammer, 2012).

²¹ Historic American Engineering Record (HAER), National Park Service, U.S. Department of the Interior, "Philadelphia, Wilmington & Baltimore Railroad, President Street Station," HAER No. MD-8.

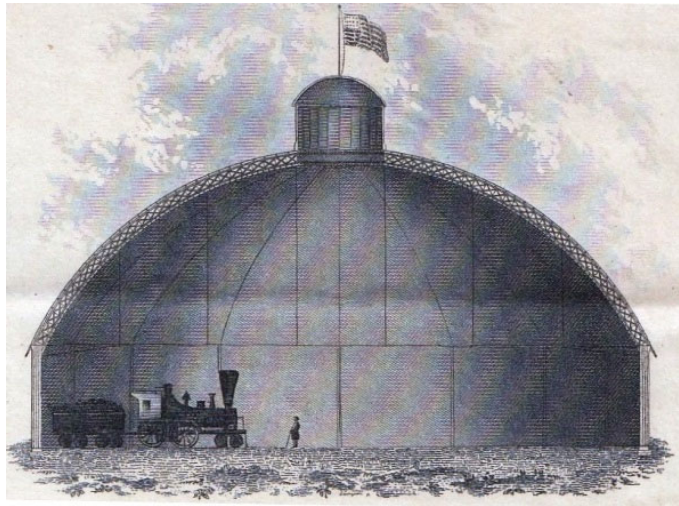


Figure 1. Roundhouse Howe truss roof. Harris & Briggs letterhead, Springfield, MA, 1856.



*Figure 2. A Howe truss supports the roof of the Cleveland Elysium ice skating rink, 1907.
Michael Schwartz Library, Cleveland State University.*

Howe trusses were also commonly used as stiffening trusses for suspension bridges, such as for the reconstruction of the Wheeling Suspension Bridge, which was severely damaged by wind in 1854. The Howe truss was sometimes incorporated with other structural forms such as bowstring bridges and portals. Figures 3 and 4 show two such applications in all-iron bridges built by the Massillon Bridge Company.²²

²² See: Historic American Engineering Record (HAER), National Park Service, U.S. Department of the Interior, "Wheeling Suspension Bridge," HAER WV-2; "Junction Road Bridge," HAER No. OH-97; and "Station Road Bridge," HAER No. OH-67.



Figure 3. Massillon Bridge Company tied arch-truss, with an all-iron Howe truss on the ca. 1875 Junction Road Bridge, Preble County, OH. HAER OH-97-4, Joseph Elliott, photographer, 1992.



Figure 4. Massillon Bridge Company portal with an all-iron Howe truss on the 1881 Station Road Bridge, Cuyahoga County, OH. All subsequent photos and charts by Dario Gasparini unless otherwise noted.

Although the Howe truss is an extraordinarily successful design, engineers have struggled to understand its structural behavior because it embodies several challenging features. It is statically indeterminate and post-tensioned, with compression-only and tension-only members, and continuous chords. Engineers have sought to resolve four principal issues:

- 1) What are the relative advantages of statically determinate versus statically indeterminate forms?
- 2) What forces are induced by tightening the rods and how should they be controlled during erection?
- 3) What are the structural implications of using compression-only (timber diagonals) and tension-only (rod) members?
- 4) What are the structural implications of using continuous chords?

Engineering judgments on these issues have changed over time and are still evolving as improved analytical models are formulated. At present, with increasing recognition of the economic and cultural value of covered bridges, two distinct approaches are used by engineers for designs of new Howe truss bridges. Perhaps the predominant approach is to use a single-diagonal, statically determinate version of the Howe truss form by using laminated wood members fastened with steel gusset plates and high strength bolts. The Charles A. Harding Memorial Bridge (World Guide to Covered Bridges no. 35-18-25), built in 1998 and designed by Richland Engineering, Ltd., of Mansfield, Ohio, represents this approach (Figure 5).²³ This is a safe, functional design, but it does not embody the key features of Howe's original patent; that is, a statically indeterminate form with post-tensioned, compression-only diagonals without "positive" connections and nodal bearings. In contrast, the Charleton Mill Bridge (World Guide no. 35-29-16#2), built in 2013 and shown in Figure 6, and the Richard P. Eastman/Hyde Road Bridge (World Guide no. 35-29-109) built in 2014, embody Howe's concepts, albeit with laminated wood sections and welded steel nodes. Smolen Engineering, Ltd., of Jefferson, Ohio, designed these two bridges. The post-tensioning was accomplished by simply tightening the nuts rather than by using load cells for control. Recently built Howe truss bridges in Switzerland and Austria generally use Howe's original design concepts almost completely.²⁴

²³ David W. Wright, editor. *World Guide to Covered Bridges*, 7th edition. (Concord, NH: The National Society for the Preservation of Covered Bridges, 2009). A single diagonal Howe is often called a "multiple king post" by the covered bridge community, but structural engineers generally do not use such a designation.

²⁴ An inventory of Swiss Howe truss bridges can be found online at "Swiss Timber Bridges," http://www.swiss-timber-bridges.ch/construction_shape/51, accessed December 12, 2018.



Figure 5. Harding Memorial Bridge (WG 35-18-25) built in 1998.



Figure 6. Charleton Mill Bridge (WG 35-29-16#2). Photo by Jack Schmidt, 2015.

There are several engineering issues in the context of covered bridge design that seek to follow Howe's original concepts:

- 1) Can a permanent pre-stress state be achieved with present-day post-tensioning technologies, and how should a desired prestress state be affected?
- 2) What prestress losses may be expected from wood viscosity?
- 3) What are the effects of temperature changes in the prestress state?
- 4) What are the long-term effects of wood hygroscopicity, and are stresses caused by moisture absorption/desorption significant?

- 5) How should the mechanism limit state capacity of a classic Howe truss, with its compression-only and tension-only prestressed members, be estimated?

The above issues are also relevant for the rehabilitation of historic Howe truss covered bridges. To improve rehabilitation techniques and inform new design, the FHWA's National Historic Covered Bridge Preservation Program decided to sponsor an in-depth research project at Case Western Reserve University (CWRU) in 2008. Christopher Marston, an architect with the Historic American Engineering Record (HAER), a division of the National Park Service (NPS)'s Heritage Documentation Programs, and project manager of HAER's National Covered Bridges Recording Project since 2002, managed the project.

In May 2004, vandals burned the short-span Howe truss railroad bridge over Moose Brook near Gorham, New Hampshire. Timothy Andrews of Barns and Bridges of New England salvaged the burnt remains of the 1918 bridge, and ownership of the remains was transferred from the state of New Hampshire to the NSPCB. The Moose Brook Bridge was a rare surviving example of a boxed Howe pony truss, and HAER decided to document the remains with measured drawings and large-format photography in the summer of 2009. Because of the bridge's manageable size and NSPCB's ownership, HAER, CWRU, and the NSPCB decided to use the Moose Brook Bridge for the Howe truss research project. Backed by FHWA funding, CWRU and the NPS signed Cooperative Agreement H2270100008 and Task Agreement J2270100010 in May 2010, with the following scope of work:

- 1) Reconstruction of the burned Moose Brook Bridge;
- 2) Instrumentation of the reconstructed bridge with strain and moisture sensors;
- 3) Controlled post-tensioning of the bridge to achieve a prescribed initial stress state
- 4) Acquisition of at least one year of strain and moisture data to determine the temporal; effects of wood viscosity and moisture and temperature variations;
- 5) Development of mathematical models for predicting time histories of forces and displacements in post-tensioned Howe trusses; and
- 6) Development of preliminary guidelines for rehabilitation of Howe covered bridges.

To carry out the first task, CWRU executed a separate agreement with the NSPCB in 2010, which in turn signed a subcontract agreement with BBofNE to do the work.

RECONSTRUCTION OF THE MOOSE BROOK BRIDGE

In 2009-2010, Timothy Andrews of BBofNE explored an extant sister bridge on the same Boston & Maine branch line, the Snyder Brook Bridge (HAER NH-49), to study the details of the Howe pony truss and its connections (see Figure 7a-b). By viewing through the access panels of the

36'-long, 4-panel Snyder Brook Bridge, Andrews confirmed the existence of counterbraces in each panel. He also found that the top of the end panel had a counter diagonal bearing on wood thrust block instead of a cast shoe. The 2004 Moose Brook fire had consumed numerous timbers, principally the truss counterbraces. Because of decades of direct contact between the wood braces and cast-iron shoes, ghost marks clearly defined the pre-fire cross sections of the lost timber members (which were of different sizes at each panel).



Figure 7a. The Snyder Brook Bridge, a boxed-in Howe pony truss. Photo by Linda Gasparini.



*Figure 7b. Snyder Brook Bridge; thrust block at top of end post and counter brace.
Photo by Christopher Marston.*

This information, combined with the 2009 HAER drawings of the Moose Brook Bridge, and previous documentation by former New Hampshire state architecture historian James Garvin,

provided sufficient information for Andrews to recreate the historic Howe pony truss and order the correct timber sizes for reconstruction.²⁵ Andrews began disassembling the Moose Brook Bridge in September 2010. However, nearly 100 years after it was first erected, the bridge's nut-bolt connections had seized up, requiring chasing the rod threads with repeated heating of the nuts, and using a rust penetrant to free up the nuts for removal (see Figure 8a). After Andrews painstakingly removed all the hardware, he loaded all the salvaged iron and steel parts as well as reusable floor beams and shipped them to a warehouse in Campton, New Hampshire for the assembly process.

Andrews had originally thought that southern yellow pine (SYP) would be the historically correct species used for the Howe truss reconstruction. However, his efforts to secure suitable sizes of SYP of the appropriate grade proved futile. After a nationwide search for any available species of timber in the required lengths, Andrews chose the Hull-Oakes Lumber Company in Monroe, Oregon, for their ability to provide the 48'-long Douglas fir timber needed for the chords.²⁶ Andrews then ordered the timber from Hull-Oakes in its various sizes on October 1, 2010. (During disassembly, it was revealed that in fact a mixture of Douglas fir and southern yellow pine had been used in the bridge.) Andrews started to season the green timbers in Campton in the last week of November 2010. By stacking the timbers outdoors and keeping them widely separated, the air-drying process could begin (see Figure 8b). The short timbers were stored inside the unheated warehouse, while the longer members remained outside in the elements to dry more slowly. After several months, the timbers were then dressed and planed to their final dimensions.

Close inspection during the disassembly process revealed cracks in five of the cast-iron thrust blocks and distortion and bends in some of the tension rods. The damage to the castings appeared to be the result of the intense heat of the fire and being quenched with water by the fire department. The project team decided that all the cracks must be repaired prior to the testing at CWRU. Alpine Machine Company, a local metal shop, straightened the steel rods at an elevated temperature between 800 and 900°F. One slightly cracked casting was fixed; however several unsuccessful attempts to repair the other castings failed. On March 25, 2011, the team contacted Vern Mesler at Lansing Community College in Lansing, Michigan. An expert on iron and steel repair techniques, Mesler had rehabilitated several historic iron and steel truss bridges, and organized annual Iron and Steel Preservation conferences. Mesler offered a new methodology for the repair, but two more attempts by Alpine proved unsuccessful. In June 2011, Mesler

²⁵ James Garvin, Sketch of Moose Brook Bridge, unpublished drawing, May 12, 1980.

²⁶ See: Historic American Engineering Record (HAER), National Park Service, U.S. Department of the Interior, "Hull-Oakes Lumber Company," HAER No. OR-89.

generously offered to try the repair the four other castings with his team of instructors at Lansing Community College.

Despite this setback, there were enough good castings, in addition to the dried and dressed Douglas fir timbers, and straightened steel rods and other historic hardware, for Andrews to finally begin the process of reconstruction of the first Howe truss, which lasted from January to May 2011.²⁷

Timothy Andrews teamed with fellow timber framer Will Truax for Barns and Bridges of New England's unique preservation project. They began with a trial layout of the truss members and castings based upon measurements obtained from forensic investigation of the charred remains. Before starting, Andrews noted that three things must happen in a Howe truss:

- 1) The diagonal braces must be square/perpendicular to the bearing faces of the cast-iron blocks;
- 2) All braces must be of the same length; and
- 3) To introduce camber, the top chord cast-iron blocks must be spaced further apart than those on the bottom chord.

To achieve these these three conditions, BBofNE arranged the cast-iron blocks on the shop floor at their theoretical locations. Inexpensive 2" x 8" framing lumber (cut to the identical lengths as the braces) was used to confirm the theoretical locations of the blocks to achieve the $\frac{3}{4}$ " camber over the length of the truss (see Figure 8c). By lofting the members on the floor, Andrews and Truax could confirm the theoretical design of the trusses. There was no room for error: no extra timbers were in the budget to allow for any miscuts or mistakes.

Then BBofNE began the process of dressing the chords. They laid out seven locations for cast-iron blocks in the bottom chord, based on the theoretical design. Then they cut housings (notches) for the cast-iron blocks and created clearance holes for the vertical rods in the chord timbers by hand, seen in Figure 9a. The bridgeworkers used saws, chisels, and a specialty tool called a scrub plane.

Starting at the two center panels, they clamped the blocks to the chords and cut the paired center diagonals (see Figure 8d). Then Andrews and Truax positioned each brace vertically above its final location using a process called "plumb line scribe" (Figure 9b). This meticulous process

²⁷ See Howe Truss Assembly Process drawing, HAER NH-48, Addendum, Sheet 4 of 8, Paul Gorokhov, delineator, 2013.

allowed the bridgewrights to measure, mark, and cut the correct location of all four corners of the diagonals for the proper square fit of the braces to the cast-iron thrust blocks. While in theory each block would have been uniform and straight, each 90-year old casting had irregularities. This became a painstaking process to fit each brace to each panel point. They eventually inserted the braces several times, checking them for fit, and then removing each one for minor tooling to achieve a 100 percent tight fit.

With the two pairs of main mid-span braces installed, and the chords properly spaced apart, the center vertical truss rod could be inserted and tightened so the process of cambering the truss could begin. The craftsmen repeated this process for each additional pair of braces until all the main braces were installed, and the design camber was established. Then they repeated the entire process of plumb-scribing, cutting, and fitting for all the single counterbraces. Finally, the team reinstalled all the main braces and counterbraces, and fully tightened the vertical rods to the chords of the Howe truss (Figure 9c).

Prior to final assembly, Andrews and Truax needed to cut and install the two pairs of two wooden end posts at each end of the truss for a total of eight posts (see Figure 9d). Then they inserted 3"-thick spacer blocks in between each chord stick and fastened them with keeper bolts. Finally, they labeled each member prior to shipment.

Andrews and Truax had completed the first truss by mid-May 2011, but it remained in New Hampshire while the team ascertained if the second truss could be assembled. After several delays to repair the broken castings, the team decided to only ship the first truss to Cleveland in August 2011 so that some preliminary testing could begin.

To prepare for transport, BBofNE then disassembled the truss one last time, and shipped the timbers and metal components on a flatbed truck to Cleveland on August 15, 2011. Andrews traveled to Cleveland to lead the team of CWRU students in reassembling the truss, shown in Figure 11a.



Figure 8a-b. Torching and grinding to loosen the bolts during disassembly of the burned timbers, October 2010. Right: Douglas fir timbers stacked for seasoning, March 2011.



*Figure 8c-d. Aligning the castings with 2 x 8s to insure perpendicular fit as part of the lofting process, February 2011. Right: Fitting the center panel braces between the top and bottom chords, March 2011.
Photos by Will Truax, 2011.*



Figure 9a-b. Handtooling square notches for the cast shoe and round notch for the tension rod. Right: Plumbline scribe.



Figure 9c-d. Scribing end posts after all braces and counters were inserted. Right: Final assembly of first truss; note timber thrust block lower lefthand corner. Photos by Will Truax, 2011.

BRAZE WELDING

After Vern Mesler generously offered to try brazing the remaining cracked castings at his Lansing Community College facility, Andrews shipped the castings in July 2011. Mesler consulted with his welding faculty members in August to come up with a repair procedure.

Preparation for the Moose Brook Bridge braze welding process began by using a dye-penetrant, non-destructive testing method to identify cracks in the cast-iron sections. Once all the cracks were identified, joint preparation began. For braze welding, joint preparation is a critical step in the process. Special attention is required for the joint profile to provide sufficient surface area for a successful braze weld.²⁸ A pneumatic hammer with a selection of sharpened chisels was used to precisely cut the braze weld joint; the action from the pneumatic hammer and chisels produced a rough surface creating a good bonding anchor pattern for the braze weld.

A steel box was fabricated to accommodate one cast-iron section at a time, along with hardwood charcoal. The casting was covered with a heat blanket and heated to about 800° F for approximately six hours to minimize thermal stresses that could lead to cracking. Once the casting reached the braze welding heat, the heat blanket was parted at the joint, and the braze welding began using Royal Tiger flux and Crown 125 (³/₈" bronze filler rod). The welding was finished while the casting remained in the firebox. The casting was then re-covered with the heat blanket and remained in the heat box until it was completely cooled. The procedures used provided a valuable case study on repair of large iron castings (see Figures 10a-f).²⁹



Figure 10a-b. Cracked casting found during disassembly, September 2010 (left). At Lansing, a pneumatic hammer was used to precisely cut the braze weld joint and produced a rough surface for good bonding.

²⁸ In braze welding, unlike electric arc welding, there is no fusion between electrode and base metal; instead, a firm bonding between the braze filler metal and base metal is essential.

²⁹ Vern Mesler email to Christopher Marston, March 27, 2019.

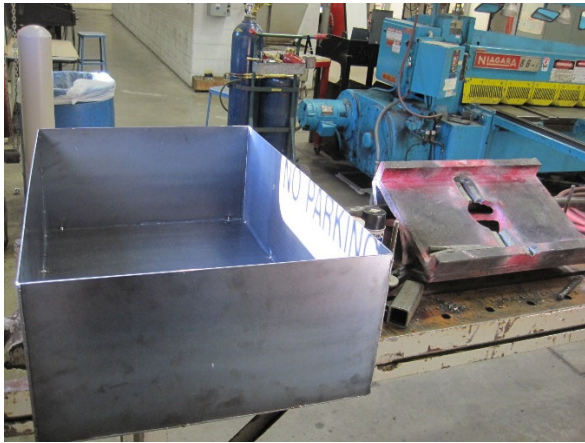


Figure 10c-d. Steel box specially fabricated to heat one casting at a time, fueled by hardwood charcoal.



Figure 10e-f. Braze welding the casting at 800°F with a bronze filler rod. Lansing Community College photos by Vern Mesler, October-November 2011.



Figure 11a. First reassembled Howe truss (West truss) of Moose Brook Bridge in Vanderhoof-Schuette Structural Laboratory at Case Western Reserve University, August 2011.

Using the repaired nodal castings and the remaining timbers and hardware, BBofNE successfully fabricated the second truss over the winter of 2011-2012, following the same painstaking process used to build the other truss. The second truss arrived at CWRU on March 16, 2012, and was reassembled on March 19 in the Vanderhoof-Schuette Laboratory (Figure 11b).



Figure 11b. Second Moose Brook Howe truss (East truss) reassembled in structural laboratory, March 2012.

INSTRUMENTATION AND POST-TENSIONING OF HOWE TRUSSES

Wood is a viscous, hygroscopic material; its stress-strain behavior is time-dependent and it absorbs/desorbs moisture. Moreover, wood and steel have different coefficients of thermal expansion. Thus, post-tensioned Howe trusses will have time-dependent strains, moisture contents, and member forces under time-varying atmospheric temperature and relative humidity conditions. Therefore, a principal research goal was to instrument the trusses, post-tension them, place them in atmospheric conditions – outside under cover – in Cleveland, Ohio, and acquire long-term data.

Forces in all members of a Howe truss may be determined by equilibrium if forces in the vertical bars are measured. Therefore, the steel bars used for post-tensioning were instrumented with weldable, full-bridge strain gauges, specifically HPI model HBWF35-1256-10GP-TR-1" PC gauges as shown in Figure 12.

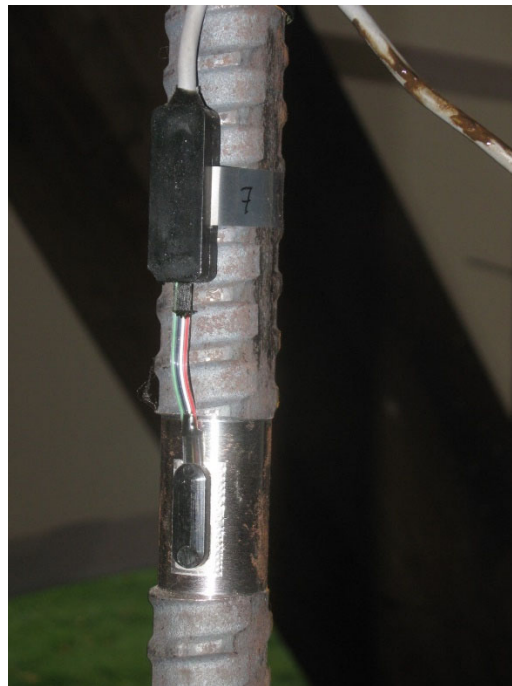


Figure 12. Weldable strain gauges on steel post-tensioning vertical bar.

The sensors were numbered as shown in Figure 13.

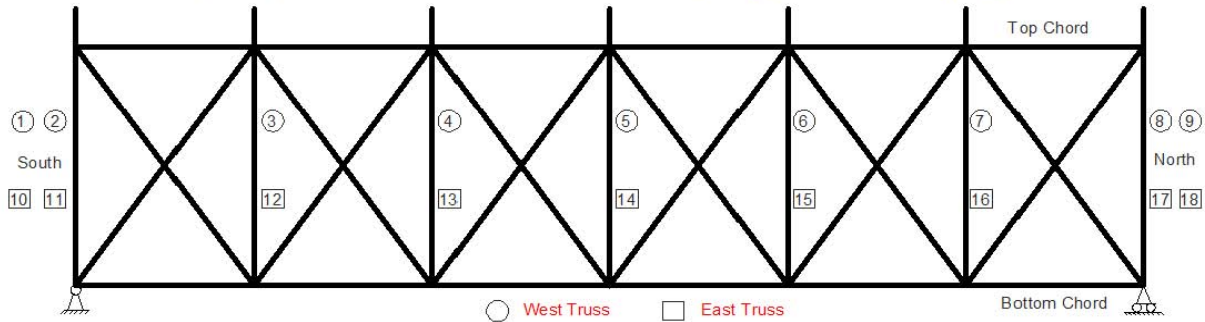


Figure 13. Numbering of strain gauges on Dywidag bars on trusses.

An objective of the research was to measure wood moisture content at various locations over a long period of time. One possible technique, such as the one developed by Brischke, Rapp, and Bayerbach, is to embed two electrodes and measure the resistance between them.³⁰ The resistance measurement must then be correlated with known moisture contents. In lieu of this, Jim Berilla, CWRU's Civil Engineering Department engineer, suggested embedding solid state temperature and relative humidity (RH) sensors. An equilibrium wood moisture content could then be computed using Equation 4-5 (the Hailwood-Horrobin equation) in the *Wood Handbook* of the Forest Products Laboratory.³¹ Berilla chose Sensirion SHT 25 sensors. These are calibrated to read temperature and RH with an accuracy of 4 percent at the extremes. The Sensirion sensors were embedded as shown in Figure 14 and sealed with an epoxy adhesive. Therefore, the sensors measured temperature and RH in a small cylindrical volume, 4 mm in diameter.

³⁰ C. Brischke, A. O. Rapp, and R. Bayerbach, "Measurement system for long-term recording of wood moisture content with internal conductively glued electrodes," *Building and Environment* 43, no. 10 (2008): 1566-1574.

³¹ *Wood Handbook: Wood as an Engineering Material*, General Technical Report FPL-GTR-190, (Madison, WI: U.S. Department of Agriculture, Forest Service, Forest Products Laboratory, 2010), 4-3.

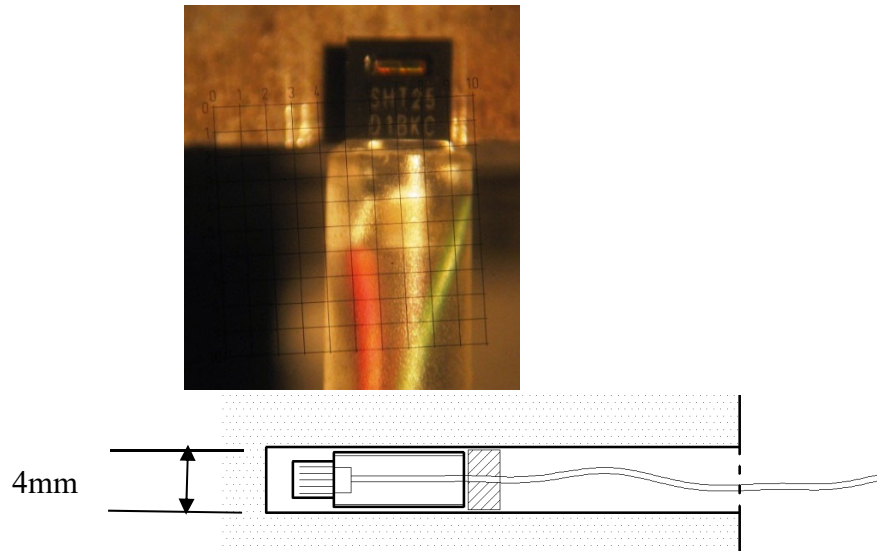


Figure 14. Sensirion SHT 25 temperature and relative humidity sensors.

To check performance, one sensor was embedded at the center of a nominal 1-1/2" cube of Douglas fir. The wood block was dried at 85° C for twenty-four hours prior to insertion of the sensor. The block with the embedded sensor was then placed in a temperature and RH controlled chamber, with the temperature maintained at 15° C and the initial RH set at 45 percent. Figure 15 shows the RH output of the sensor versus time. After moisture diffused into the wood to nearly equilibrium conditions, the sensor RH reading was 43.3 percent. The chamber RH set point was then raised to 70 percent and the sensor, again after some time to achieve equilibrium, also rose to 70 percent RH. Therefore, in equilibrium conditions the RH in the small cylindrical volume in which the sensor is embedded equals the RH at the boundary of the wood. Using Equation 4-5 in the *Wood Handbook*, the equilibrium moisture content in the wood increased from 8.6 percent to 13.3 percent as the chamber RH was increased from 45 percent to 70 percent (at a constant temperature of 15° C).³² A total of fourteen Sensirion SHT 25 sensors were deployed in the wood members.

³² *Wood Handbook*, 4-3.

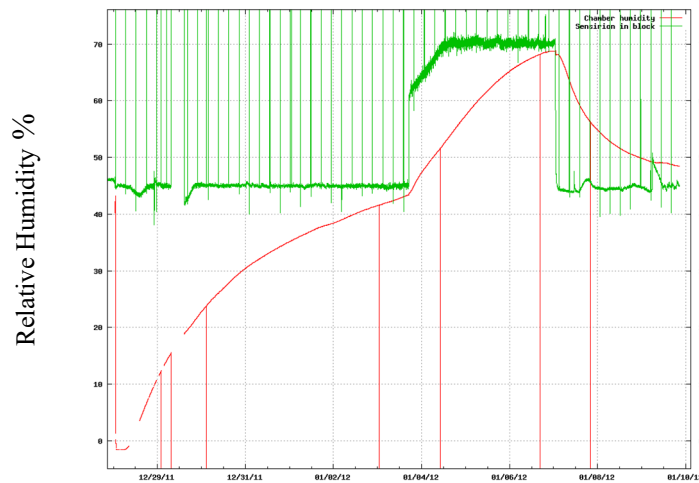


Figure 15. Sensirion SHT 25 RH reading and chamber RH reading versus time.

To post-tension the Howe trusses, all the original steel threaded rods were replaced with high strength, 1"-diameter, Dywidag bars instrumented with strain gauges. In addition, the original end conditions of the trusses were modified by removing the wood endposts and 1"-diameter tension rods and replacing them with two Dywidag bars placed outside the wood thrust blocks, as shown in Figure 16a-b. (Note that the Case research team named the trusses “East” and “West” after moving them outside in September 2012.) First, they moved the 2012 reconstructed truss outside, and placed it nearest to the lab or west side. Then they moved the truss reconstructed in 2011 and placed it on the east side.



Figure 16a-b. Original and modified end panel conditions of Moose Brook Bridge Howe trusses.

Post-tensioning of the 2012 truss with repaired castings (West truss) – The second reconstructed truss was delivered to CWRU on March 16, 2012, with repaired cast-iron nodes. Post-tensioning on this truss was performed on June 13, 2012, using the setup shown in Figure 17.



Figure 17. Post-tensioning setup using two 60-ton jacks from a single hydraulic manifold.

As post-tensioning forces were gradually increased, bearing failures were noticed in the wood thrust blocks at the truss ends. Therefore, steel bearing channels and backup steel angles were added as shown in Figure 18 and 19.



Figure 18. Added steel bearing channels.



Figure 19. Added steel backup angles.

Figure 20 shows the Dywidag bar forces, labeled 1 to 9, versus time for the period from June 13-25, 2012. Initial forces in the interior bars varied from 76 to 82 kips. These values decreased about 20-25 percent over two weeks because of the viscous behavior of the wood. It is important to emphasize that the prestress force caused stresses normal to the grain in the two chords and it is likely that these stresses caused most of the losses. This behavior was quickly recognized by

early builders, who then devised cast-iron tubular sleeves extending through the chord thickness, effectively eliminating stresses normal to the grain.³³

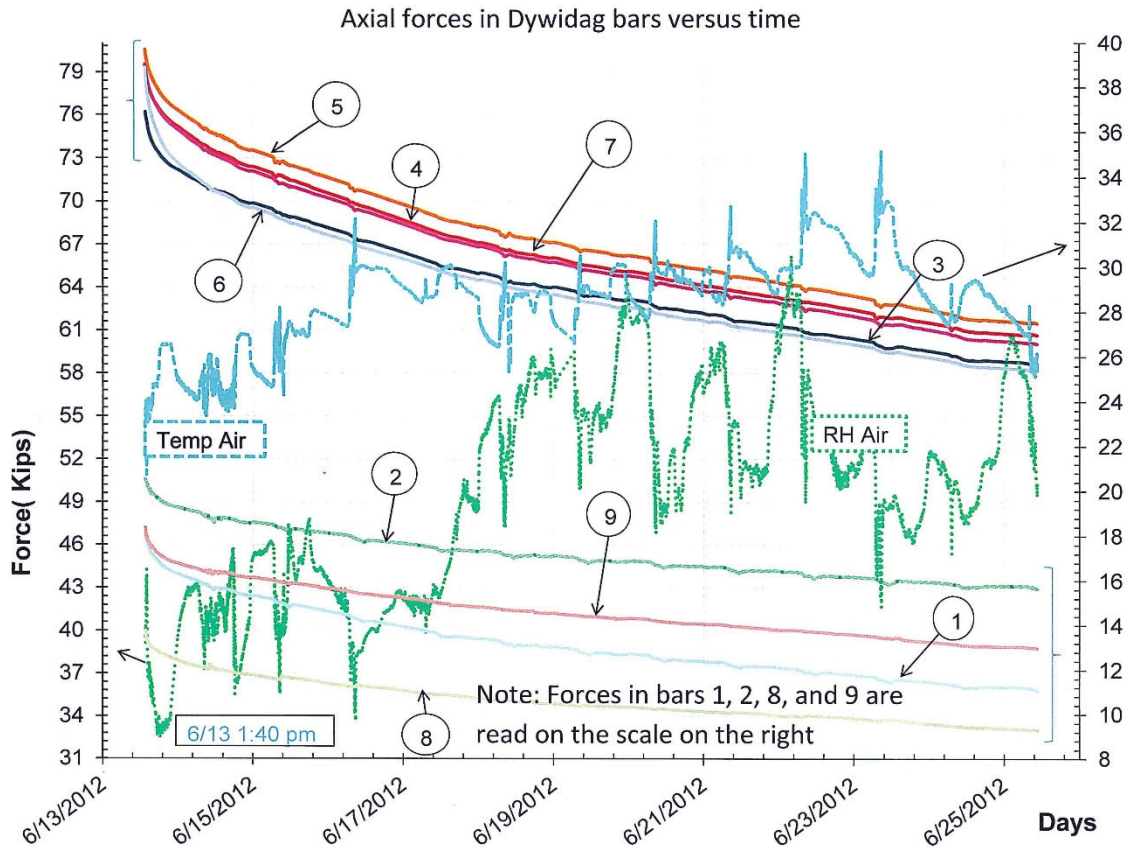


Figure 20. Axial forces in Dywidag bars 1 to 9 versus time.

³³ D. A. Gasparini, J. Bruckner, and F. da Porto, "Time-Dependent Behavior of Posttensioned Wood Howe Bridges," *ASCE Journal of Structural Engineering* 132, no. 3 (March 2006): 419.

Post-tensioning of the 2011 truss with original castings (East truss)—Next, the Case team prepared the 2011 or East truss for post-tensioning by removing all the wood end posts and replacing all the original steel tension rods with instrumented Dywidag bars. On removal of the wood end posts, however, the top chord twisted and moved laterally as shown in Figure 21a-c.

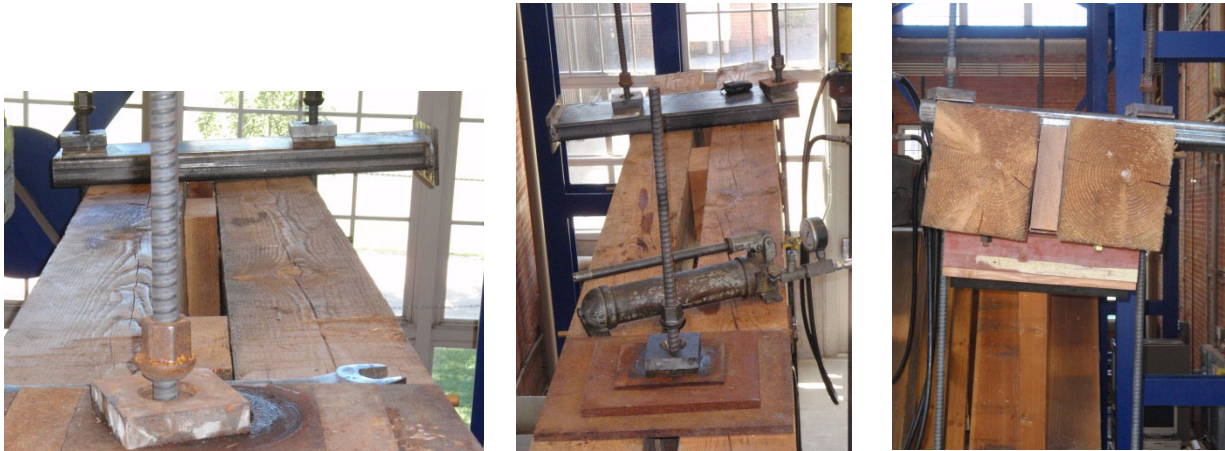


Figure 21a-c. Twist and lateral motion of top chord of the West truss.

Therefore, prior to post-tensioning, the team tried to decrease the twist and lateral displacement of the ends of the top chord using a screw jack and a post as shown in Figures 22 and 23.



Figure 22. Screw jack to decrease chord twist.



Figure 23. Post to decrease chord twist.

Because of the twist and lateral motion of the top chords, the two Dywidag bar forces at the end nodes were very different. Post-tensioning on the East truss began on June 14, 2012. As forces were increased, the central casting on the lower chord cracked as shown in Figures 24 and 25.



Figure 24. Cracked casting at middle node. Figure 25. New crack in middle casting of bottom chord.

A visual and photographic inspection revealed an old crack in the casting with surface corrosion, as shown in Figure 26. It is likely that this undetected, pre-existing crack weakened the casting.



Figure 26. Detail of pre-existing crack showing surface corrosion in the middle bottom chord casting.

To repair the crack, two end plates were put in place and tightened with two 1-¼" steel bolts, as shown in Figures 27 and 28. Because of the cracked casting and the twist in the top chord, it was decided to limit the prestress of the East truss to approximately one-half that of the West truss.



Figure 27. Repair of cracked casting.



Figure 28. Repair of cracked casting.

Figure 29 shows time histories of the Dywidag bar forces in the East truss for the period from June 14-25, 2012. The bars are numbered 10 to 18. Again, viscous wood behavior caused a decrease in the member prestress forces.

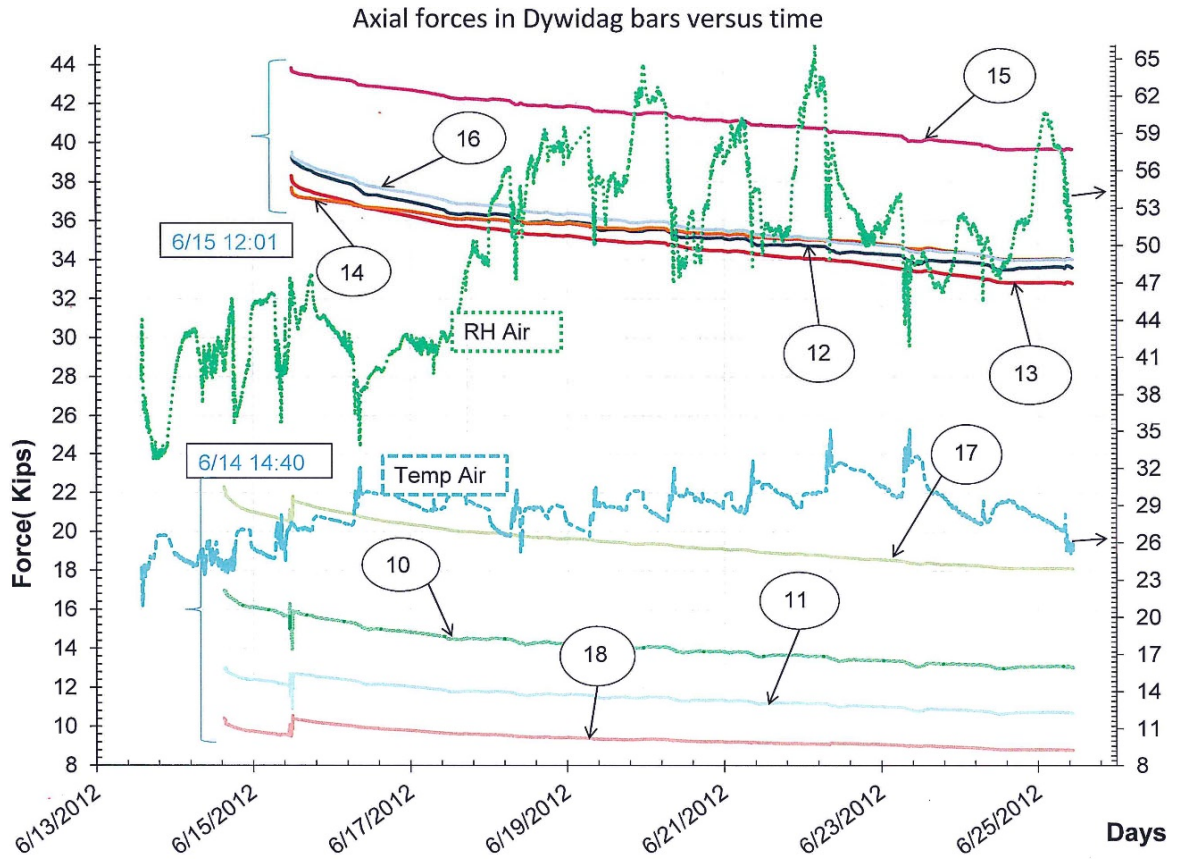


Figure 29. Axial forces in Dywidag bars 10 to 18 versus time.

INSTRUMENTATION AND POST-TENSIONING OF AN 8"X8" DOUGLAS FIR SPECIMEN

An 8" x 8" Douglas fir specimen was instrumented and post-tensioned as shown in Figure 30 to help the team gain experience before working on the actual trusses.



Figure 30. Post-tensioning an 8"x8" Douglas fir specimen.

The 8" x 8" timber was post-tensioned on April 3, 2012, and placed outdoors on May 7, 2012, as shown in Figure 31. The initial sum of the forces in the two bars was approximately 50,000 lbs, producing an initial compressive axial prestress in the wood of approximately 950 pounds per square inch (psi). Three Sensirion temperature (T) and relative humidity (RH) sensors were embedded in the wood, one at the center of the section, another at quarter depth, and one near the surface (about a centimeter from the surface). Atmospheric T and RH sensors were also deployed. A data acquisition system recorded data at a rate of two samples per minute. Figure 32 shows wood compressive stress data recorded from the time of initial prestressing to June 25, 2012. Viscous wood behavior caused a slow decrease in the compressive prestress of about 6 percent in the first month. This decrease is much smaller than that observed on the West truss because the 8" x 8" post-tensioned specimen had no stresses normal to the grain. Noticeable daily force fluctuations occurred after the specimen was placed in an outdoor environment. These fluctuations are due to the different coefficients of thermal expansion of steel and wood.



Figure 31. Prestressed 8" x 8" Douglas fir specimen in its outdoor enclosure.

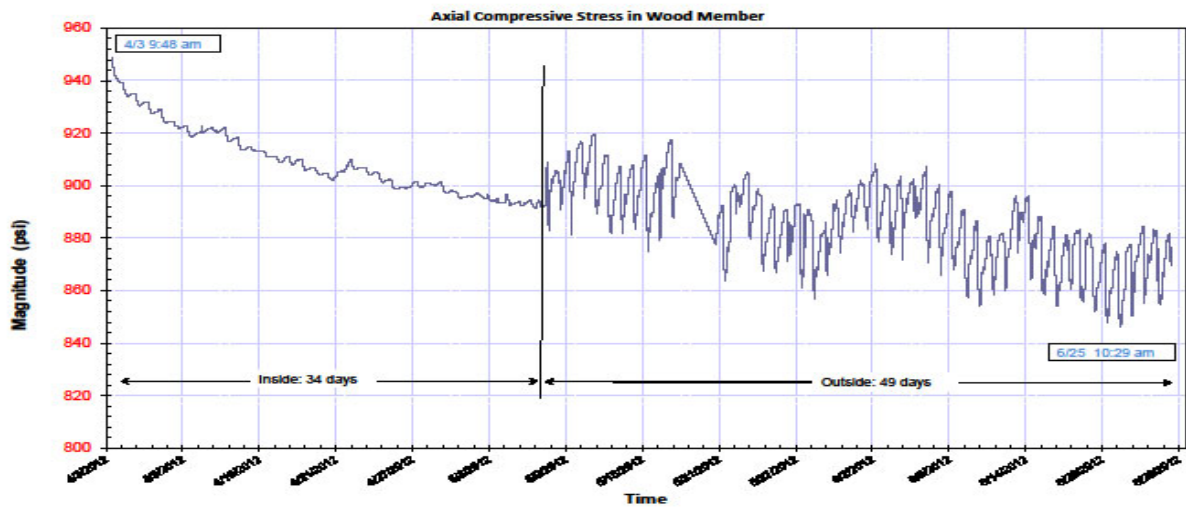


Figure 32. Axial stress in 8" x 8" Douglas fir specimen versus time.

OUTDOOR INSTALLATION OF HOWE TRUSSES AND ERECTION OF PROTECTIVE COVER

Figure 33 shows the conceptual design of the cover for the two trusses. It consisted of four steel arches covered by an architectural fabric manufactured by the Seaman Corporation of Wooster, Ohio. Seaman manufactured and fabricated the architectural fabric on a pro-bono basis for the research project at CWRU.

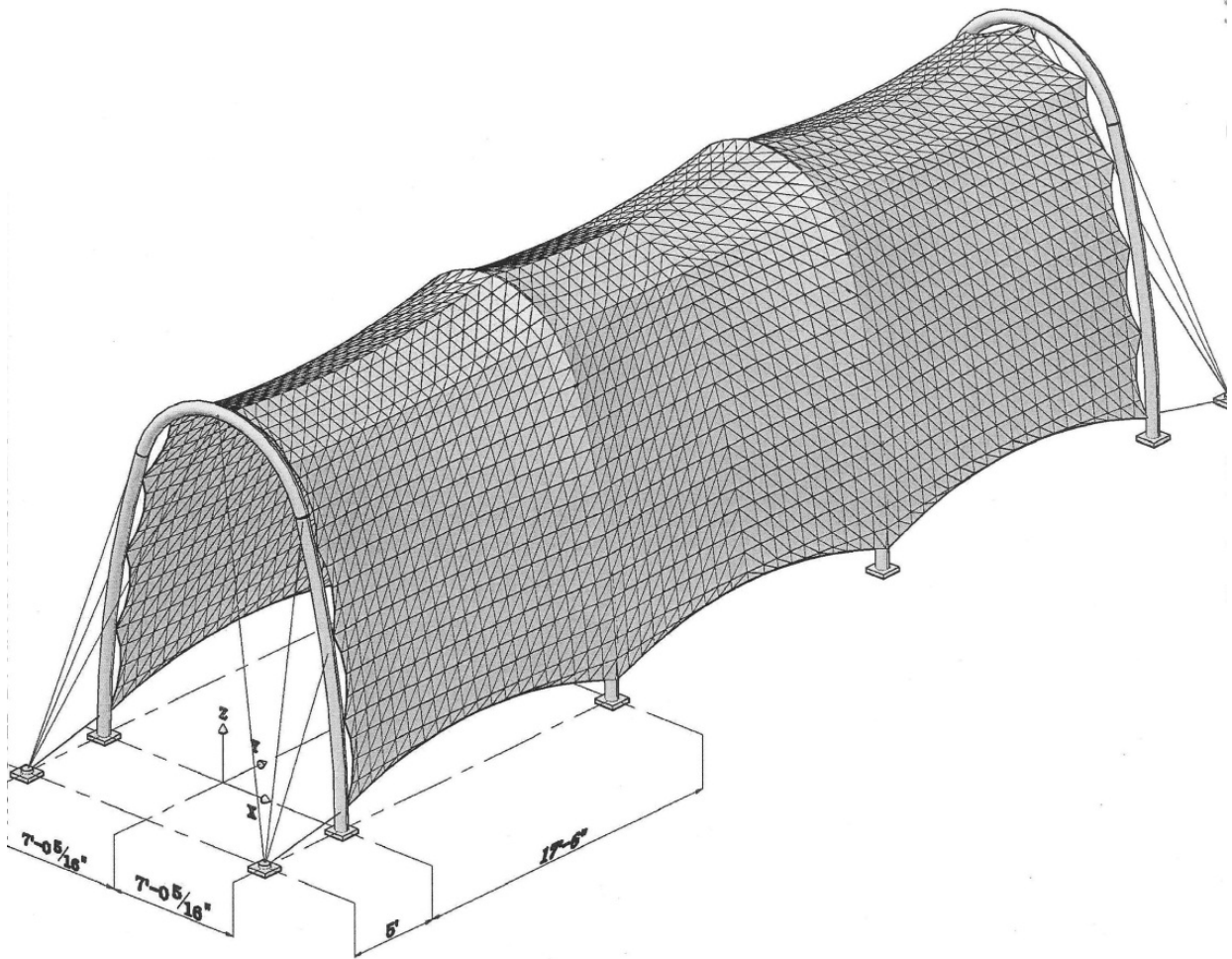


Figure 33. Conceptual design of cover for Howe trusses. Drawing by Pavel Gorokhov, 2012.

Fabrication of the steel arches for the protective cover and installation of the foundations for the arches required extensive work, which was performed in-house. A rigger moved the trusses outdoors on September 25, 2012. Figures 34 and 35 show the transfer of the trusses to outside of the Vanderhoof-Schuette Structural Laboratory.



Figure 34. Moving the trusses outdoors, September 25, 2012.



Figure 35. Outdoor installation of steel arch frames over Howe trusses. Note the East truss, reconstructed in 2011, positioned in the foreground. The West truss is behind, closest to the lab.

The protective cover shown in Figure 36 was erected beginning on October 3, 2012.



Figure 36. Protective cover for Howe trusses.

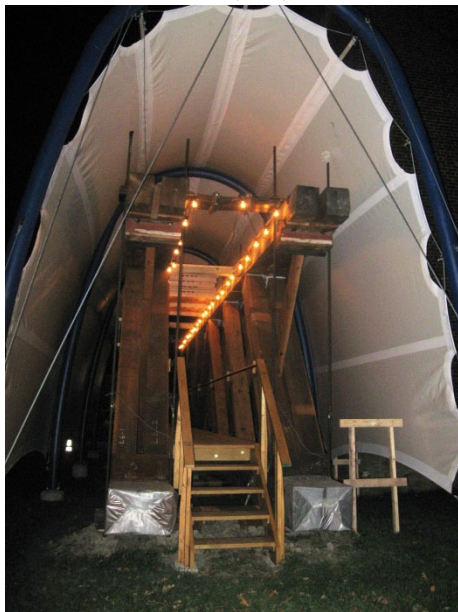
The installation was completed in November 2012, after the team installed a floor, railings, stairs, and lights. Six interpretive signs were fabricated and hung. The installation was completely open to the public as shown in Figure 37.



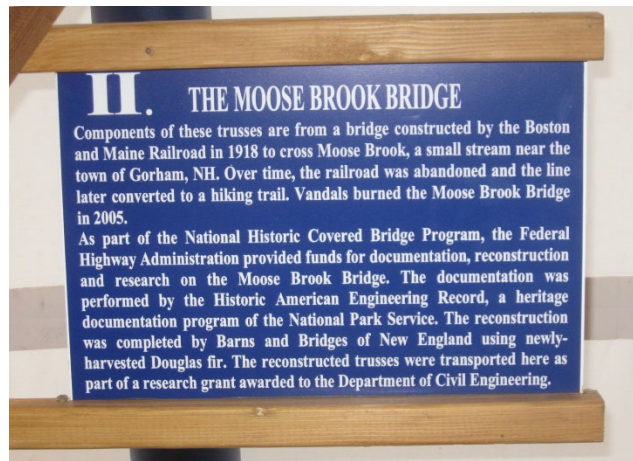
(37a)



(37b)



(37c)



(37d)

Figure 37a-d. Outdoor installation of Howe truss exhibit, open to the public.

MATHEMATICAL MODELING

The design of a Howe truss must at least consider the post-tensioning action, dead load, live load, and temperature variations. The immediate effects of post-tensioning may be determined by linear elastic models, with effective nodal loads from the prescribed prestrains in the steel or wrought-iron rods. Because wood is viscous, axial forces and displacements will vary with time. It should be emphasized that the post-tensioning action does not produce a pure creep (constant stress) or a pure relaxation (constant strain) condition; both stresses and strains vary with time. Temporal changes in the effects of post-tensioning may be predicted by linear viscoelastic models.³⁴ In 2006, Gasparini, Bruckner, and daPorto presented the governing equations for linear viscoelastic models of trusses, for both three-parameter solid and Burger linear viscoelastic material models. Linear viscoelastic models may be represented graphically in one dimension by different combinations of linear elastic “spring elements” and linear viscous “dashpot elements.” Figure 38a-b shows two models for the post-tensioned 8" x 8" system shown in Figure 31. The steel rods are assumed to be linear elastic; the Burger model for wood has an additional linear dashpot element with parameter μ_1 .

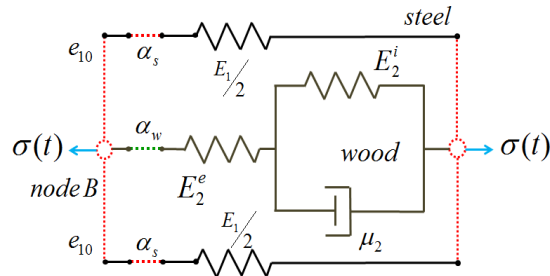


Figure 38a. Linear model for the post-tensioned system of Fig. 31; linear elastic model for steel; three-parameter-solid linear viscoelastic model for wood.

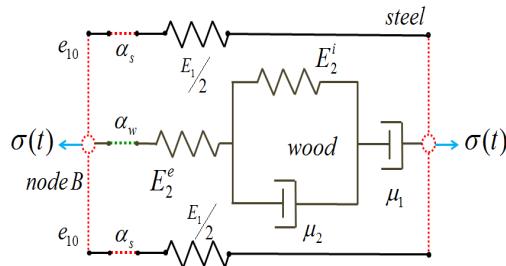


Figure 38b. Linear model for the post-tensioned system of Fig. 31; linear elastic model for steel; Burger linear viscoelastic model for wood.

³⁴ Gasparini, Bruckner, and daPorto, “Time-Dependent Behavior.”

The relative predictions of the two models depends strongly on the ratio μ_1/μ_2 . Figure 39 shows the predicted decrease in the initial post-tensioning force in the system of Figure 31 for three values of μ_1/μ_2 . The assumed viscoelastic parameters were those given by Fridley for Douglas fir. An important observation is that most of the losses from viscoelastic behavior occur within the first few months. The three-parameter-solid model predicts that the long-term force will reach an asymptotic value. The Burger model predicts a finite, constant, long-term rate of decrease. If $\mu_1/\mu_2 = 10,000$, the two predictions are practically equal and the long-term constant rate of decrease for the Burger model is extremely small. In fact, for Douglas fir, $\mu_1/\mu_2 \approx 10,000$.³⁵

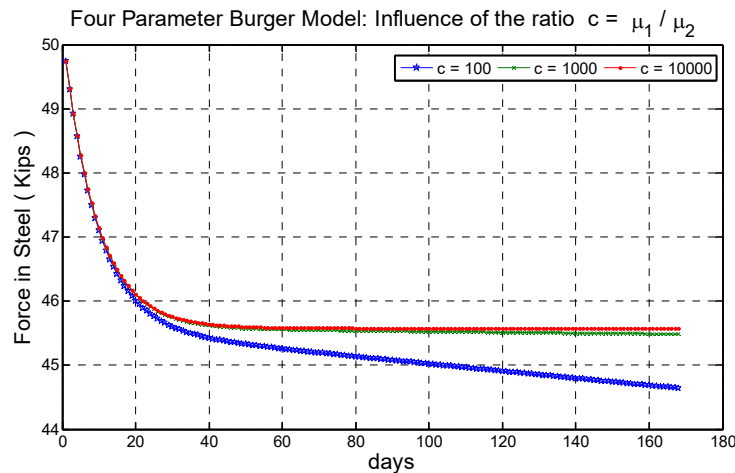


Figure 39. Predicted loss of prestress from linear viscoelasticity for system shown in Figure 31.

Linear viscoelastic parameters for wood are functions of temperature and moisture content, and its rate of change. Moreover, there is considerable statistical variability in the values, even within one species. Therefore, a range of values should be used to bound possible long-term behavior.

An important observation made by Gasparini, Bruckner, and daPorto is that smaller stiffness, high-strength rods with larger initial prestrains will produce prestress states that will be less affected by wood viscosity.³⁶ Figure 40 shows the predicted behavior of the post-tensioned 8" x 8" Douglas fir if bars of three different diameters (and relative axial stiffnesses) are used to produce the same initial prestress force. The long-term decrease in prestress force is only 8.6 percent if 5/8"-diameter bars are used, whereas the loss is 17.7 percent if 1-1/4" diameter bars are used.

³⁵ K. J. Fridley, "Designing for creep in wood structures," *Forest Products Journal* 42, no. 3 (1992): 23-28.

³⁶ Gasparini, Bruckner, and daPorto, "Time-Dependent Behavior."

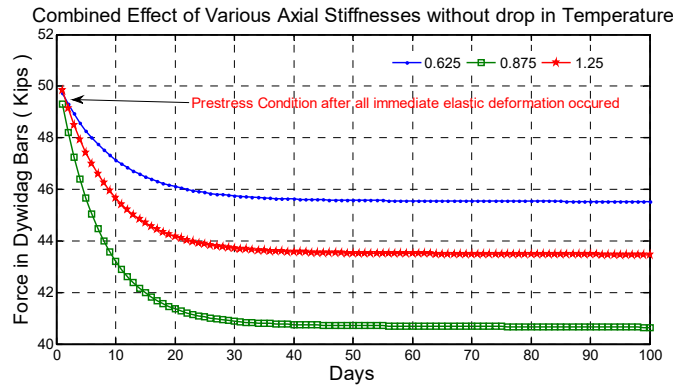


Figure 40. Loss of prestress in system of Figure 31 for three bar diameter values.

Linear elastic models may be used to predict the effect of transient live loads and the immediate effects of temperature changes. If a temperature change is sustained, temporal changes in prestress will occur because of wood viscosity. Figure 41 shows the predicted behavior of the 8" x 8" system if a sudden, but sustained, temperature *decrease* of 40° F occurs.

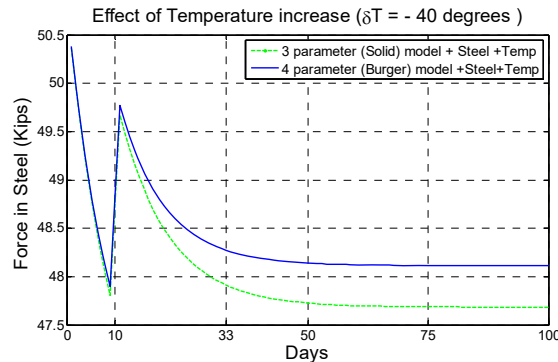


Figure 41. Effect of a 40°F **decrease** in temperature on the post-tensioned system of Figure 31.

Because of differences in the coefficients of thermal expansion, an approximate 4 percent increase in the prestress force occurs. In the same way, if there is a temperature *increase*, the prestress force will decrease. Therefore, it seems desirable to prestress during warm temperatures. Of course, atmospheric temperatures have diurnal and yearly seasonal variations, therefore a post-tensioned system will have corresponding force fluctuations as recorded in Figure 32.

Wood is a hygroscopic material; that is, moisture moves in and out of wood. As the wood moisture content changes, shrinkage/swelling strains occur. These strains are anisotropic; that is, they are different in the tangential, radial, and longitudinal directions of the wood. Does this hygroscopic behavior affect forces and displacements in prestressed structural systems such as

Howe trusses in an outdoor environment? If so, how may this behavior be modeled mathematically and what are the magnitudes of the effects? Are the effects significant for design? In this context, some relevant basic concepts are as follows:

Dew point temperature – The temperature to which air with a given water vapor content and pressure must be cooled to become saturated with water vapor. A state of saturation exists when the air contains the maximum amount of water vapor possible at the existing temperature and pressure. When further cooled, the airborne water vapor will condense to form liquid water.

Relative Humidity (RH) – The ratio of vapor pressure in air at a certain temperature to the saturation vapor pressure in air at the same temperature, expressed as a percent.

Wood moisture content (MC) – The amount of water contained in wood, expressed as a percentage of the mass of oven-dried wood. The *Wood Handbook* of the Forest Products Laboratory states that moisture content may be calculated by:

$$MC = \frac{m_{wet} - m_{dry}}{m_{dry}} (100)$$

In which m_{wet} denotes the mass of the wood before oven drying. Because the oven-dry mass is almost always used as the basis, the MC can exceed 100 percent. When wood is first cut, it is said to be green. Table 4-1 in the *Wood Handbook* gives average moisture content for green wood of various species. The MC of green wood “can range from about 30% to more than 200%.”³⁷ Green wood must generally be air-dried (seasoned) or kiln-dried to decrease the green moisture content and thus minimize shrinkage strains and maximize dimensional stability during usage.

Wood fiber saturation point (MC_{fs}) – Moisture can exist in wood as “free water” within wood cells and cavities and/or as “bound water” within the cell walls. The moisture content at which the cell walls are completely saturated but no “free water” exists is called the fiber saturation point, MC_{fs}. As noted in the *Wood Handbook*, “the fiber saturation point is considered as the moisture content above which the physical and mechanical properties of wood do not change as a function of moisture content. The fiber saturation point of wood averages about 30% moisture content, but in individual species and individual pieces of wood it can vary by several percentage points from that value.”³⁸

³⁷ *Wood Handbook*, 4-1 to 4-2.

³⁸ *Wood Handbook*, 4-2.

Wood equilibrium moisture content (EMC) – For any given temperature and RH, wood equilibrium moisture content is defined as the moisture content at which there is no ingress/egress of moisture in the wood. Table 4-2 in the *Wood Handbook* gives EMC as a function of temperature and RH, “which may be applied to wood of any species.”³⁹ The table was computed using an equation proposed by Hailwood and Horrobin with parameters computed by Simpson.⁴⁰ For example, at a temperature of 70° F and a RH of 55 percent, the EMC is 10.1 percent. EMC increases as RH increases and decreases as temperature increases. Simpson provided data on monthly EMC’s in 262 outdoor location in the U.S. For Cleveland, Ohio, the EMC varies only 2 percent over the year, from 12.6-12.8 percent in April through July to 14.6 percent in November and December. By contrast, in Fresno, California, the EMC varies 8.8 percent over the year, from 7.8 percent in July to 16.6 percent in December.⁴¹

Wood shrinkage/swelling strains – As previously noted, changes in moisture content cause shrinkage/swelling strains that are anisotropic. Table 4-3 in the *Wood Handbook* lists radial, tangential, and volumetric shrinkage strains (expressed as a percent of the green dimension) for a large set of domestic woods. The transverse and volumetric shrinkage values have a coefficient of variation of approximately 0.15.⁴² Shrinkage/swelling is greatest in the tangential direction, about 1.5 to 2 times the shrinkage/swelling in the radial direction. Coast Douglas fir has 7.6 percent tangential shrinkage and 4.8 percent radial shrinkage. Longitudinal (parallel to the grain) shrinkage is much smaller; according to the *Wood Handbook*, “average values for [longitudinal] shrinkage from green to oven-dry are between 0.1% and 0.2% for most species of wood.”⁴³ This implies that shrinkage/swelling from changes in moisture content may be less significant for trusses, in which the axial direction of the members is invariably the longitudinal direction of wood, although radial and tangential strains in the chords can also affect member axial forces.

Mechano-sorptive effects – It has been observed that changes in moisture content affect the time-dependent deformations of wood under load and, conversely, that applied stresses can affect the shrinkage/swelling behavior from changes in moisture content. The interactions between moisture content changes and applied stress are called “mechano-sorptive” phenomena. To predict such phenomena, the mathematical models for predicting moisture content changes must

³⁹ *Wood Handbook*, 4-3.

⁴⁰ A. J. Hailwood and S. Horrobin, “Absorption of water by polymers: Analysis in terms of a simple model,” *Transactions of the Faraday Society* 42 (1946): 84-102; William T. Simpson, “Predicting Equilibrium Moisture Content of Wood by Mathematical Models,” *Wood and Fiber* 5, no. 1 (Spring 1973): 41-49.

⁴¹ W. T. Simpson and J. Y. Liu, “An Optimization Technique to Determine Red Oak Surface and Internal Moisture Transfer Coefficients During Drying,” *Wood and Fiber Science* 29, no. 4 (October 1997): 312-318.

⁴² *Wood Handbook*, 4-6.

⁴³ *Wood Handbook*, 4-5.

be formulated jointly, or be “coupled with,” models for mechanical stress.⁴⁴ A principal implication of these coupled models is that the predictions from de-coupled linear viscoelastic models and moisture diffusion models, which are briefly discussed next, have greater uncertainty.

Motivated primarily by the need to understand and optimize the process of drying wood, researchers have modeled moisture movement within wood extensively.⁴⁵ The primary model used is Fickian diffusion, whose basic assumption is that the rate of transfer of a “diffusant” (moisture in the case of wood) is proportional to the gradient of the diffusant concentration times a diffusion coefficient, D , assumed to be a material property.⁴⁶ The basic isotropic, two-dimensional (in X-Y space) Fickian diffusion model is given by the partial differential equation:

$$D\left(\frac{\partial^2 C}{\partial x^2} + \frac{\partial^2 C}{\partial y^2}\right) = \frac{\partial C}{\partial t}$$

In which,

t = time

C = Concentration of diffusant (water content); a function of x and y

D = Diffusion coefficient

To solve the equation, initial concentrations (moisture contents) at time $t = 0$ must be assumed throughout a cross-section, and boundary conditions must also be assumed. A common assumed boundary condition is:

$$D\frac{\partial C}{\partial x} = S(C_b - C_e(t))$$

⁴⁴ R. H. Leicester, “A Rheological Model for Mechano-sorptive Deflections of Beams,” *Wood Science and Technology* 5 (1971): 211-220; David G. Hunt and Christopher F. Shelton, “Progress in the analysis of creep in wood during concurrent moisture changes,” *Journal of Materials Science* 22, no. 1 (1987): 313-320; A. Mårtensson, “Mechano-sorptive effects in wooden material,” *Wood Science and Technology* 28, no. 6 (1994): 437-449; M. Houška and Pino Koc, “Sorptive Stress Estimation: An Important Key to the Mechano-Sorptive Effect in Wood,” *Mechanics of Time-Dependent Materials* 4 (March 2000): 81-98; J. M. Husson, F. Dubois, and N. Sauvat, “Elastic response in wood under moisture content variations: analytic development,” *Mechanics of Time-Dependent Materials* 14, no. 2 (2010): 203-217.

⁴⁵ A. B. Newman, “The Drying of Porous Solids: Diffusion and Surface Emission Equations,” *Transactions of the American Institute of Chemical Engineers* 27 (1931): 203-211; Simpson, “Predicting Equilibrium Moisture Content of Wood”; R. Baronas, F. Ivanauskas, I. Juodeikienė, and A. Kajalavičius, “Modeling of Moisture Movement in Wood during Outdoor Storage,” *Nonlinear Analysis: Modeling and Control* 6, no. 2 (2001): 3-14.

⁴⁶ J. Crank, *The Mathematics of Diffusion*, 2nd ed. (Oxford: Clarendon Press, 1975).

In which,

S = Surface emission coefficient

C_b = Moisture concentration in the wood at its boundary

$C_e(t)$ = Moisture concentration in equilibrium with atmospheric conditions

The above equation also serves as a model for *moisture transmission across a boundary* of the wood. It states that the concentration gradient at a boundary is proportional to the difference between the moisture concentration in the wood at its boundary and the concentration that would be in equilibrium with the atmospheric temperature and RH conditions. The surface emission coefficient, S, controls the rate at which moisture is transmitted across a boundary. $S = 0$ implies an impermeable surface; that is, a wood surface wrapped or coated with an impervious cover. There is extensive literature on estimation of the diffusion coefficient, D, and the surface emission coefficient, S.⁴⁷ It has been determined that D is a function of position within a tree, orientation at a point, species, temperature, moisture content, and its spatial gradient. That is, D is not a unique material property of wood. Heartwood has a different D than sapwood. D in the longitudinal direction is much larger than D in the radial and tangential directions. D increases as temperature and moisture content increase. The surface emission coefficient, S, is sensibly a function of ambient air velocity.⁴⁸ Common values of D for wood are:

10^{-10} – 10^{-11} m²/sec (1.34×10^{-2} – 0.134×10^{-2} in²/day); values for S are typically 10^{-7} – 10^{-8} m/sec (3.4×10^{-1} – 0.34×10^{-1} in/day).

Initial moisture content conditions within a wood cross-section are generally unknown. Sensirion SHT 25 temperature and RH sensors could be embedded at various depths within a cross-section, and the resultant point equilibrium moisture contents computed by using Equation 4-5 of the *Wood Handbook* could be used to fit an initial moisture content function for an entire cross-section.⁴⁹

⁴⁷ C. Skaar, "Analysis of Methods for Determining the Coefficient of Moisture Diffusion in Wood," *Journal of Forest Products Research Society* 4, no. 6 (1954): 403-410; E. T. Choong and C. Skaar, "Separating internal and external resistance to moisture removal in wood drying," *Wood Science* 1 (1969): 200-202; W. T. Simpson and J. Y. Liu, "An Optimization Technique to Determine Red Oak Surface and Internal Moisture Transfer Coefficients During Drying," *Wood and Fiber Science* 29, no. 4 (October 1997): 312-318; Joseph A. M. Fotsing, and Claude W. Tchagang, "Experimental determination of the diffusion coefficients of wood in isothermal conditions," *Heat Mass Transfer* 41 (September 2005): 977-980.

⁴⁸ Howard N. Rosen, "The Influence of External Resistance on Moisture Adsorption Rates in Wood," *Wood and Fiber Science* 10, no. 3 (Fall 1978): 218-228.

⁴⁹ *Wood Handbook*, 4-3.

Outdoor temperature and relative humidity vary throughout the year. Therefore the equilibrium concentration, C_e , varies with time. Recorded atmospheric temperature and relative humidity values may again be used with Equation 4-5 in the *Wood Handbook* to compute time histories of wood moisture contents in equilibrium with the measured atmospheric conditions. It then follows that the diffusion equation must be solved for the computed time histories, $C_e(t)$.⁵⁰

In reality the diffusion equation cannot be solved analytically for a general cross-sectional shape and a complex time history, $C_e(t)$. Rather, finite difference or finite element numerical formulations must be used. Truss members usually have rectangular cross-sections with two axes of symmetry; therefore, if the initial moisture content distribution also has the same two axes of symmetry, a solution over one quadrant is sufficient. In summary, because of uncertainties in D , S , the initial moisture content, and $C_e(t)$, there is considerable variability in moisture diffusion predictions. The presence of knots, checks, and splits adds to this variability.

To increase understanding of moisture diffusion, some preliminary numerical studies were performed as follows: constant atmospheric conditions were assumed with $C_e = 14.6\%$ equilibrium water content. This value was computed using Equation 4-5 in the *Wood Handbook* from the initial recorded atmospheric temperature and RH values when the post-tensioned system shown in Figure 30 was first installed outdoors. The initial moisture content distribution within the cross-section was assumed to be that shown in Figure 42. It was estimated from Sensirion temperature and RH values at three depths within the 8" x 8" cross-section when the system was first installed outdoors.⁵¹

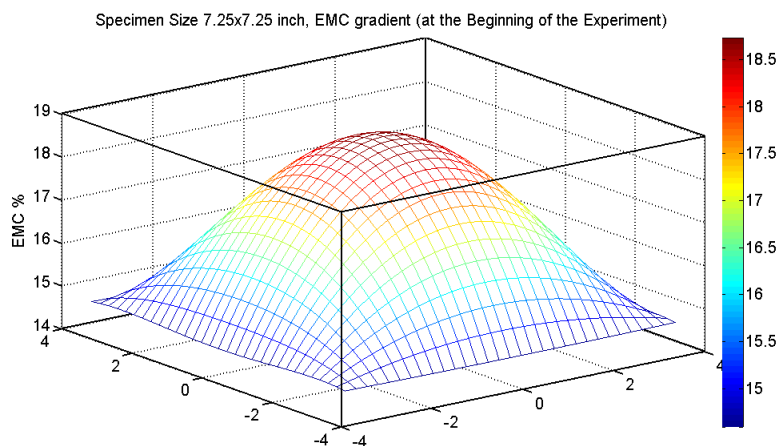


Figure 42. Assumed initial moisture content distribution within the cross-section.

⁵⁰ *Wood Handbook*, 4-3.

⁵¹ *Wood Handbook*, 4-3.

Given the particular assumed initial and boundary conditions, diffusion of moisture occurred from the center of the cross-section to the boundaries. A two-dimensional finite difference numerical formulation was implemented in MATLAB to solve the diffusion equation. Two cross-section sizes and a range of values for D and S were used.

Figure 43 shows moisture contents at the surface, quarter point, and midpoint for two cross-sections as a function of time; $D = 1.12 \times 10^{-2} \text{ in}^2/\text{hour}$ and $S = 0.112 \text{ in}/\text{hour}$. Since the initial moisture content at the boundary was equal to the assumed C_e it did not vary with time. The quarter and midpoint moisture contents asymptotically decrease to $C_e = 14.6$; for this particular parameter set, the moisture content in the 8" x 8" cross section reached the boundary value in approximately fifty days, whereas for the 12" x 12" it took approximately 150 days.

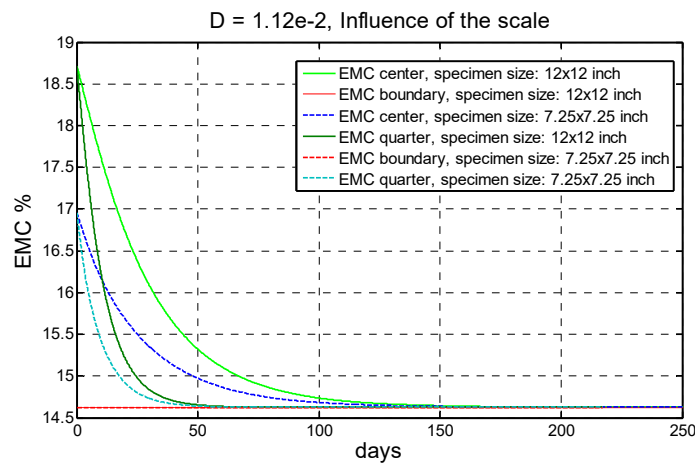


Figure 43. Time histories of moisture content at three points for two cross section sizes.

Figure 44 shows the moisture content at three points in the 8" x 8" section for three different values of D with $S = 0.112 \text{ in}/\text{hour}$. For $D = 0.56 \times 10^{-2} \text{ in}^2/\text{hour}$, the quarter and midpoint moisture contents reached the boundary value in approximately 100 days, while for $D = 2.24 \times 10^{-2} \text{ in}^2/\text{hour}$, the boundary moisture content was reached in approximately thirty days.

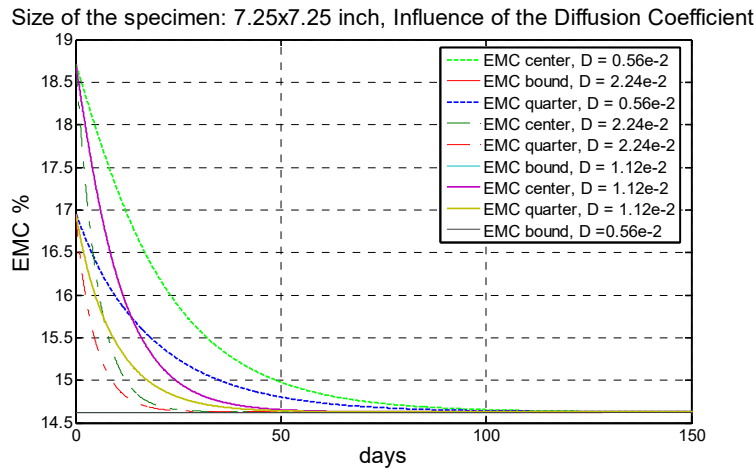


Figure 44. Influence of the diffusion coefficient on the time histories of moisture content.

Figure 45 shows the influence of the surface emission coefficient on the time histories of moisture content. Recall that $S = 0$ means an impervious boundary with no emission/ admission of moisture through such a boundary. As $S > 0$ decreases, it takes a longer time to reach the boundary concentration, $C_e = 14.6$. For $S = 0$, the moisture content becomes uniform within the cross-section at $C = 16.5$ percent.

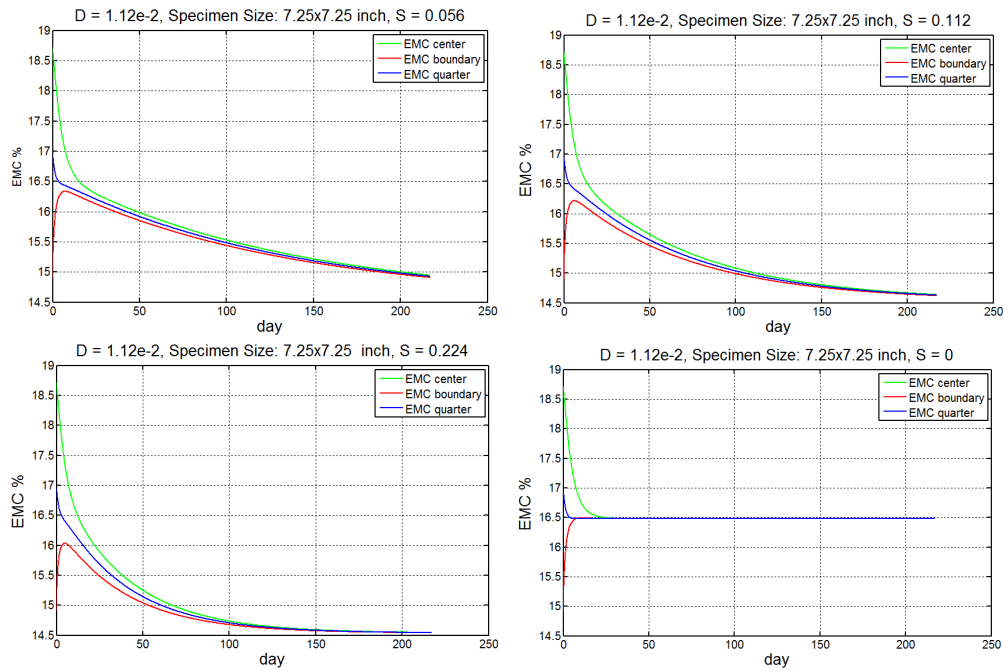


Figure 45. Influence of surface emission coefficient, S , on the time histories of moisture content.

DATA, ANALYSES, AND OBSERVATIONS

The system shown in Figure 31 and the trusses were installed outdoors in Cleveland, Ohio. Figures 46, 47 and 48 provide an indication of Cleveland weather. They show atmospheric temperature and RH data recorded at Cleveland Hopkins International Airport, on the west side of Cleveland, for the year 2010. Figure 46 indicates that the range in atmospheric RH is smaller in the winter, primarily because the minimum RH is larger at the lower temperatures in the winter. Figure 46 shows daily maximum and minimum temperatures. No minimum temperatures below 0° F were recorded for this particular year, but below 0° F temperatures commonly occur in Cleveland. High temperatures during the summer seldom reach 100° F. Figure 48 shows daily average RH and temperature (in °C) data. Average RH tends to be higher in the winter and summer and lower in the spring and fall. As previously noted, Simpson stated that for Cleveland, Ohio, the wood EMC varies only 2 percent over the year, from 12.6-12.8 percent in April through July to 14.6 percent in November and December.⁵²

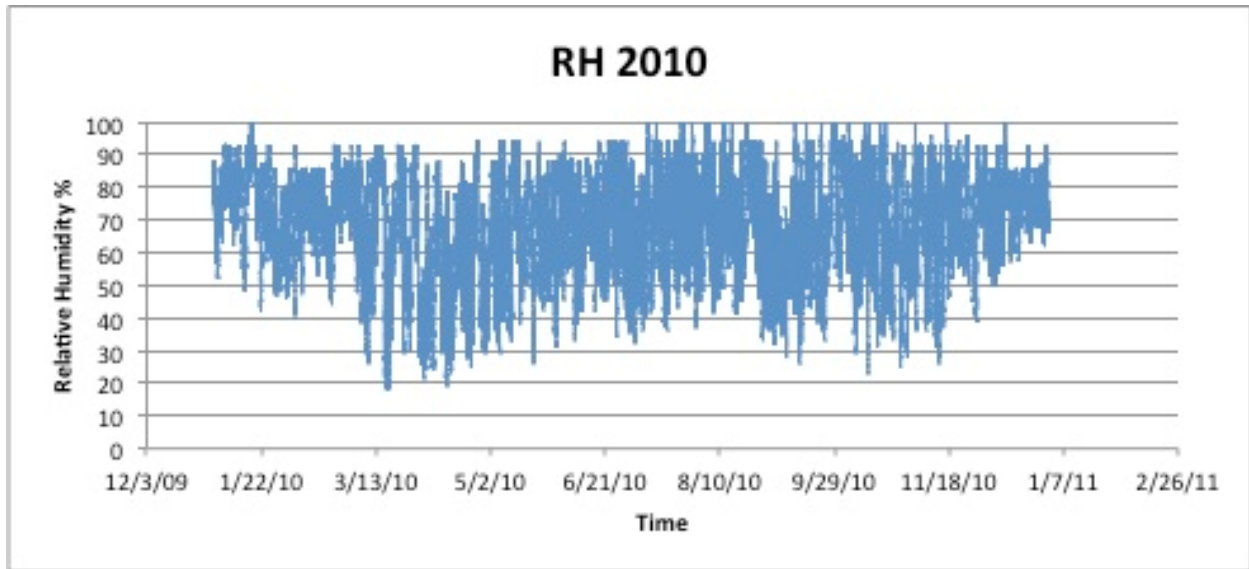


Figure 46. Cleveland Hopkins Airport Relative Humidity vs. Time in 2010.

⁵² William T. Simpson, "Equilibrium Moisture Content of Wood in Outdoor Locations in the United States and Worldwide," Research Note FPL-RN-0268 (Madison, WI: U.S. Department of Agriculture, Forest Service, Forest Products Laboratory, 1998).

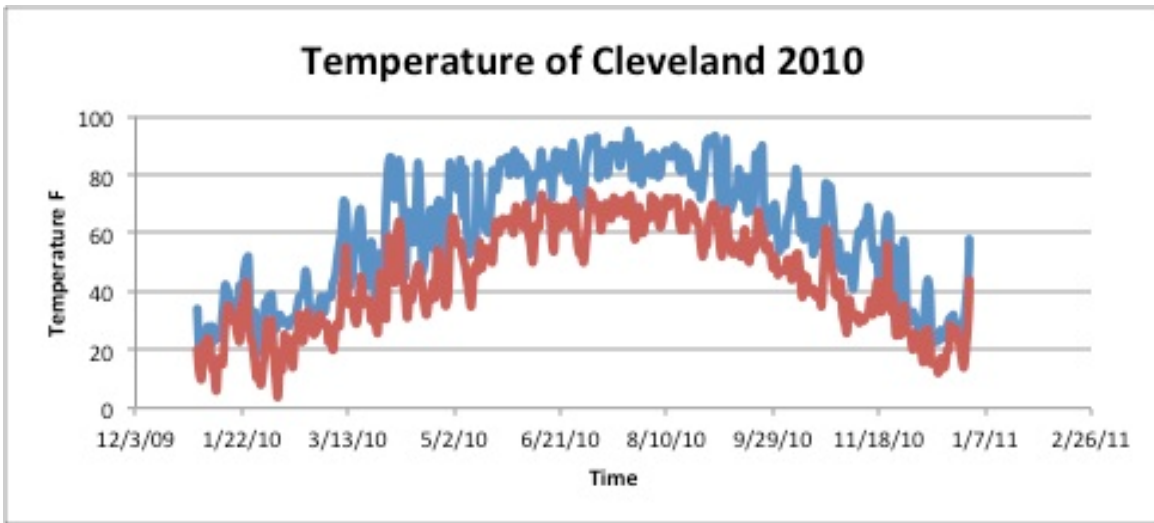


Figure 47. Daily Maximum and Minimum Temperatures in Cleveland in 2010.

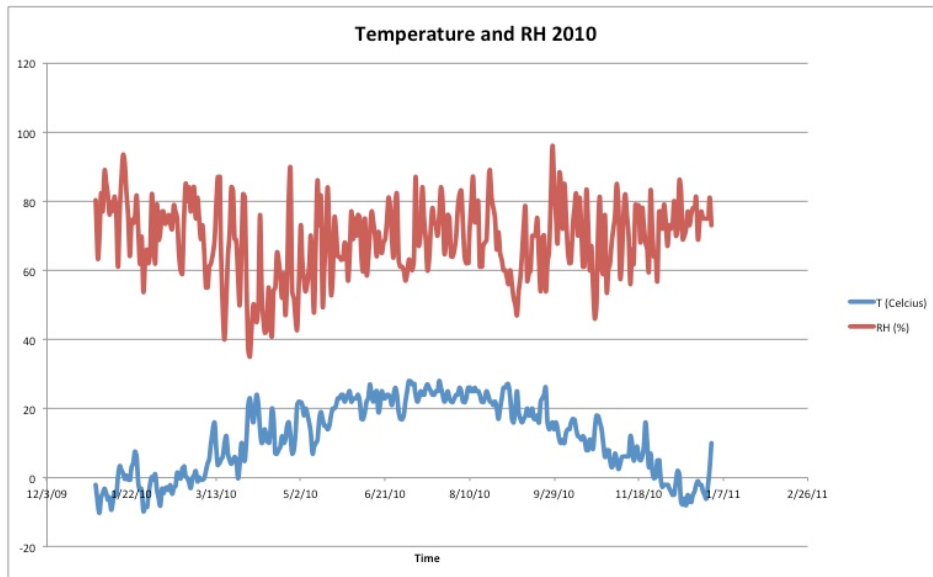


Figure 48. Daily Average Temperature and Relative Humidity vs. Time for the year 2010.

Date	Event
4/3/2012	System post-tensioned in laboratory
5/7/2012	System installed outdoors as shown in Figure 31
10/26/2012	Start of over six days of heavy rains from hurricane Sandy
7/27/2016	System installed in a controlled temperature and RH box; T=26°C; RH ≈ 96%
12/20/2017	End of data acquisition

Table 1. Timeline for significant events for post-tensioned system shown in Figure 31.

8" x 8" post-tensioned system shown in Figure 31 – Table 1 provides a timeline for the significant events related to the post-tensioned system shown in Figure 31. In addition to the strain gauges installed on the Dywidag bars to control post-tensioning forces, there were five Sensirion SHT 25 sensors installed to measure temperature and RH. One was installed within a solar radiation shield to measure atmospheric temperature and RH; a second was installed in the center of a loose 1" cube of Douglas fir. In addition, three were installed at three different depths in the 8" x 8" as shown in Figure 49.

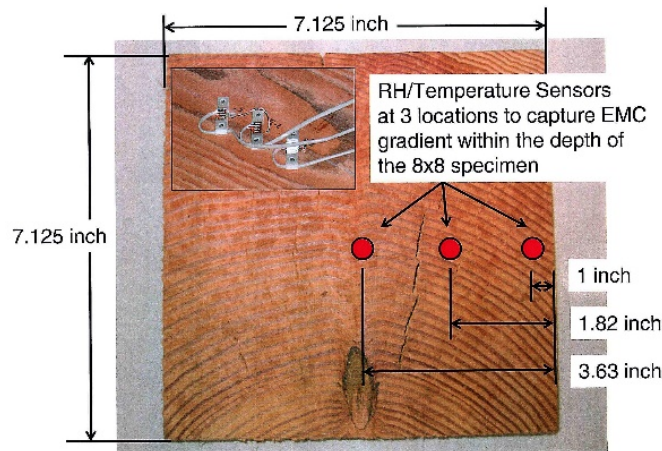


Figure 49. Sensirion SHT 25 sensors installed at three different depths of the 8" x 8" member.

The long-term data acquisition system was designed, built, and maintained by Jim Berilla, a Civil Engineering Department engineer at CWRU. The sampling rate was 2 per minute or at a time interval of 30 seconds. This sampling rate enabled the capture of daily, monthly, and yearly phenomena. Figure 50 shows time histories of five sensor readings for a period of over five years.

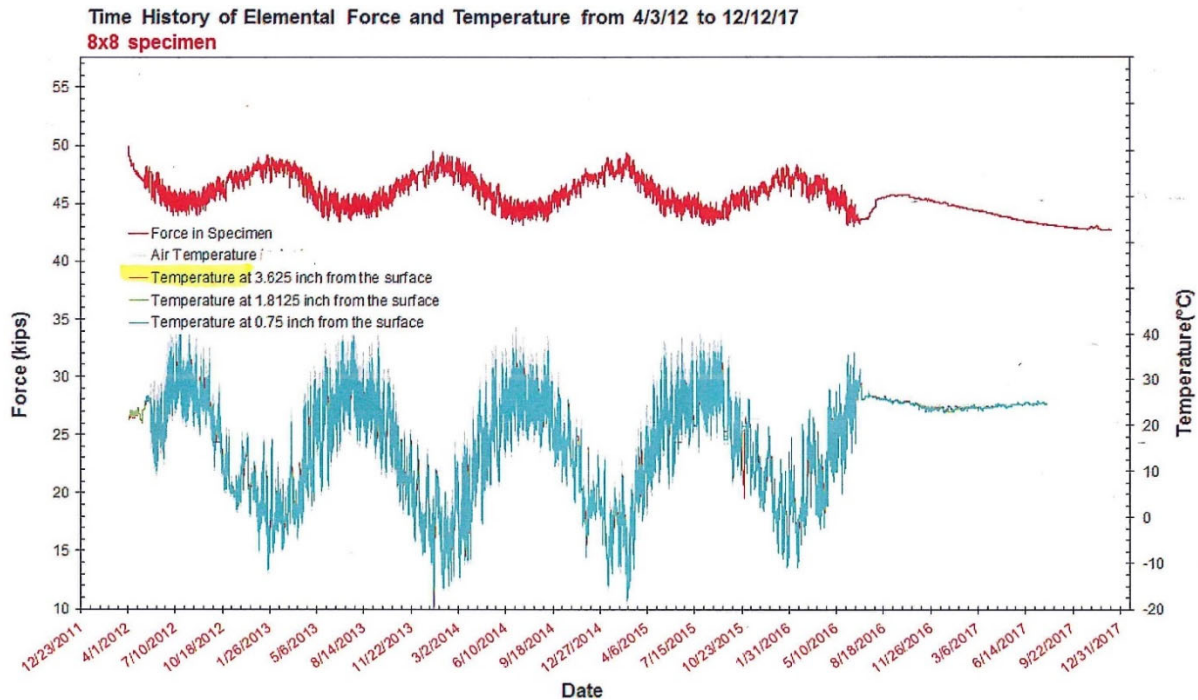


Figure 50. Force and temperature time histories.

There was no significant interruption during the data acquisition period. The data offers remarkable testimony to the long-term reliability of the sensors and of the data acquisition system. The wood member axial force versus time plot together with the details given in Figure 32, show that practically all the prestress loss from wood viscosity occurred in the first few months. There is no significant prestress loss over the following four and a half years. The axial force has a yearly cycle in inverse correspondence to the atmospheric temperature because of the different coefficients of thermal expansion of wood and steel. The yearly fluctuations have a range of approximately 10 percent. At the scale shown there is no evident difference between the atmospheric temperature and the three temperatures at the various depths of the 8" x 8" member. When the system was placed in a box with a controlled temperature of 26° C and a controlled RH of \approx 96%, the axial force first rose slightly and then decreased, possibly because of greater wood viscosity at the constant elevated RH. The Sensirion sensors failed in July 2017, after about one year in the box with temperature equal to 26° C and RH \approx 96%.

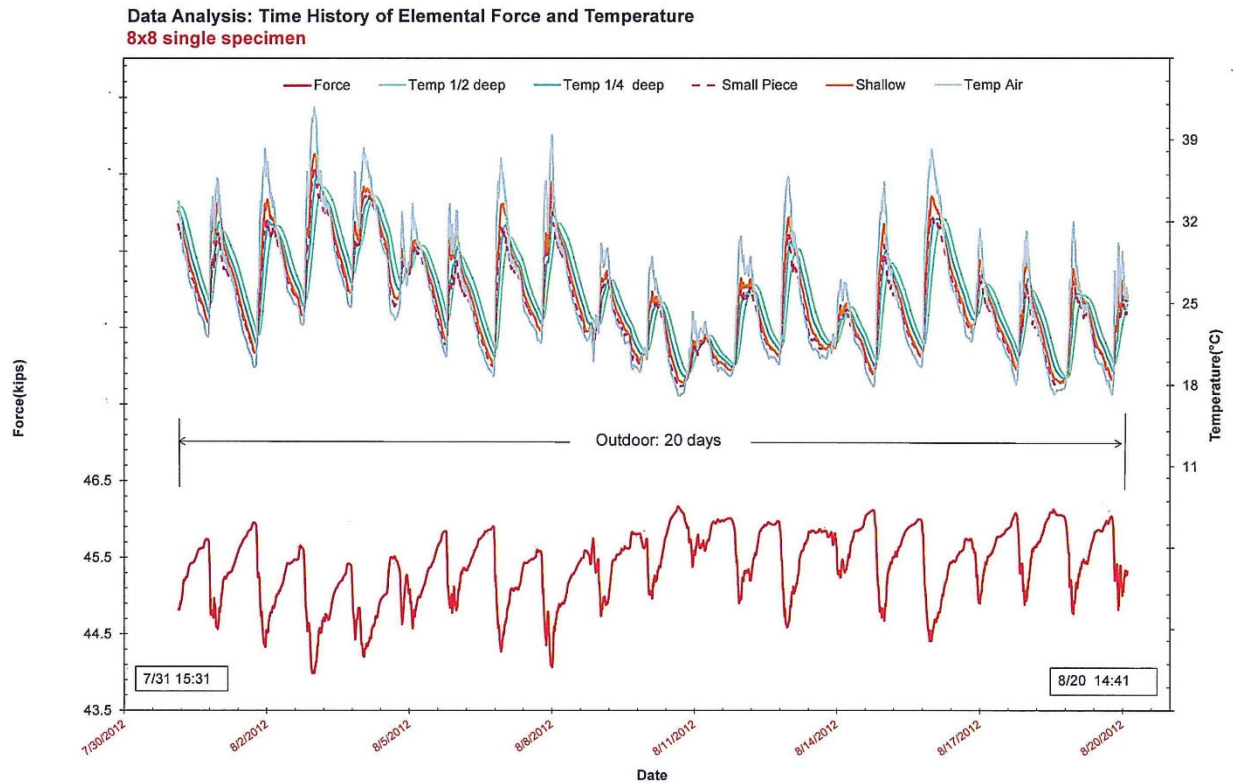


Figure 51. Time histories of force and temperatures for a period of twenty days.

Figure 51 shows six time histories at a finer scale, encompassing about twenty summer days. The data show a daily range in force of approximately 3.5 percent. The finer temperature time histories indicate that the 8" x 8" generally has smaller maximum temperatures than the peak atmospheric temperatures. There are small temporal phase lags between the temperatures at the three different depths of the 8" x 8" and the atmospheric temperature. That is, temperatures at the various depths reach their maxim after the peak atmospheric temperature occurs.

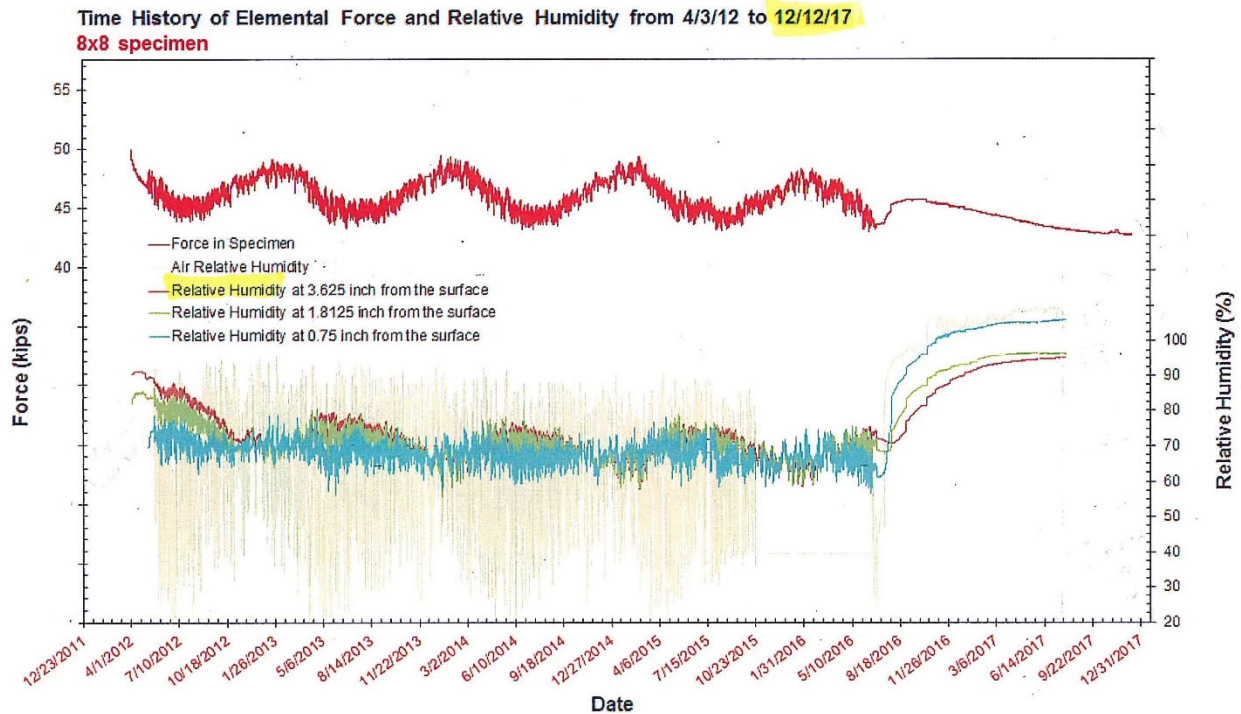


Figure 52. Time histories of force and relative humidity.

Figure 52 shows the same time history of member force and four relative humidity time histories. In agreement with the Cleveland Hopkins Airport data, the minimum values of atmospheric RH are smaller in the spring and fall and larger in the summer and winter. Note that the RH at the midpoint of the 8" x 8" began at a higher value than those nearer the surface. The RH ranges in the wood are much smaller than the range in atmospheric RH. As noted, the Sensirion sensors failed in July 2017. For some time before the failures, two of the RH sensors gave false RH values of slightly above 100 percent. Figure 53 provides finer time histories of RH values over a period of twenty summer days. The RH at mid-depth is practically constant at 80 percent. The range is greater near the surface of the 8" x 8" and the range at the center of the small 1" cube follows the atmospheric RH fluctuations closely. Figure 54 shows time histories of temperature and RH over a period of approximately two years and eight months. The minimum and maximum RH values at mid-depth of the 8" x 8" are approximately 65 percent and 80 percent with smaller values occurring in winter months. Figure 55 shows time histories over a one-year period. The RH at mid-depth is slightly larger than the RH near the surface of the 8" x 8" in late spring and summer and then is practically equal to the RH near the surface in fall and winter.

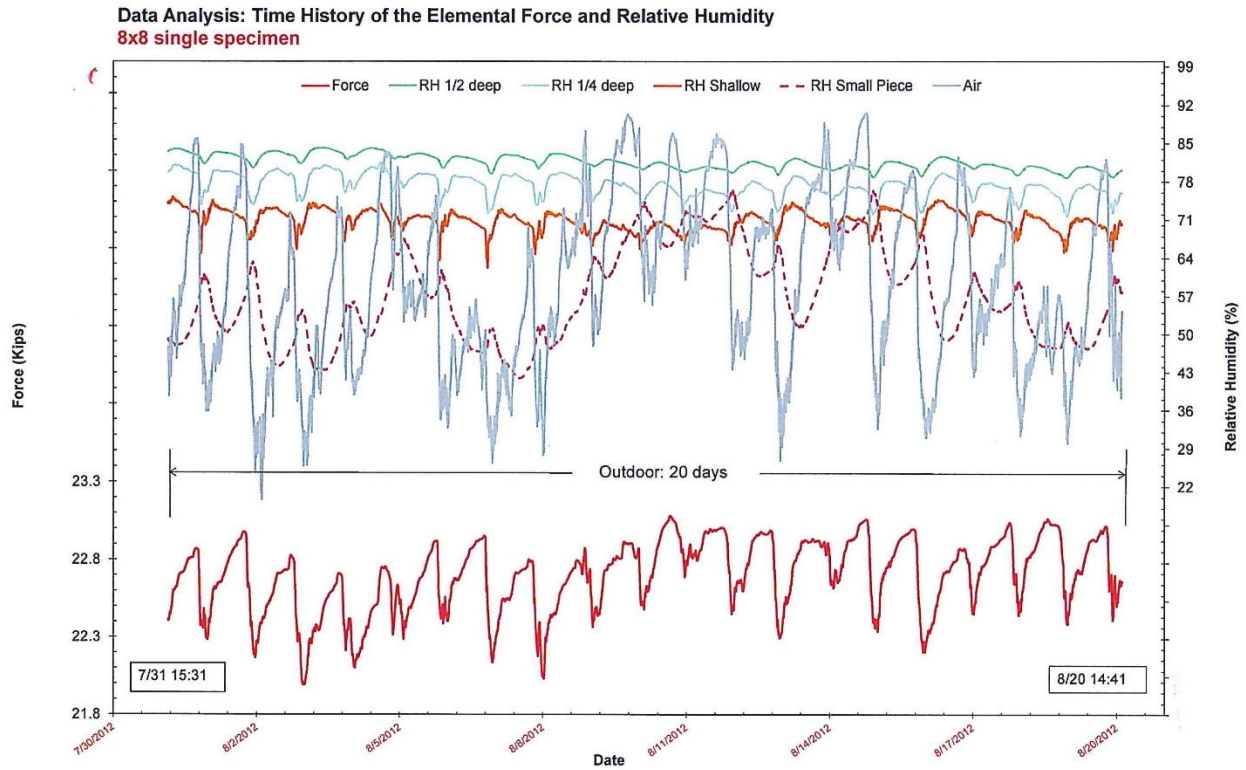


Figure 53. Time histories of force and RH over twenty summer days.

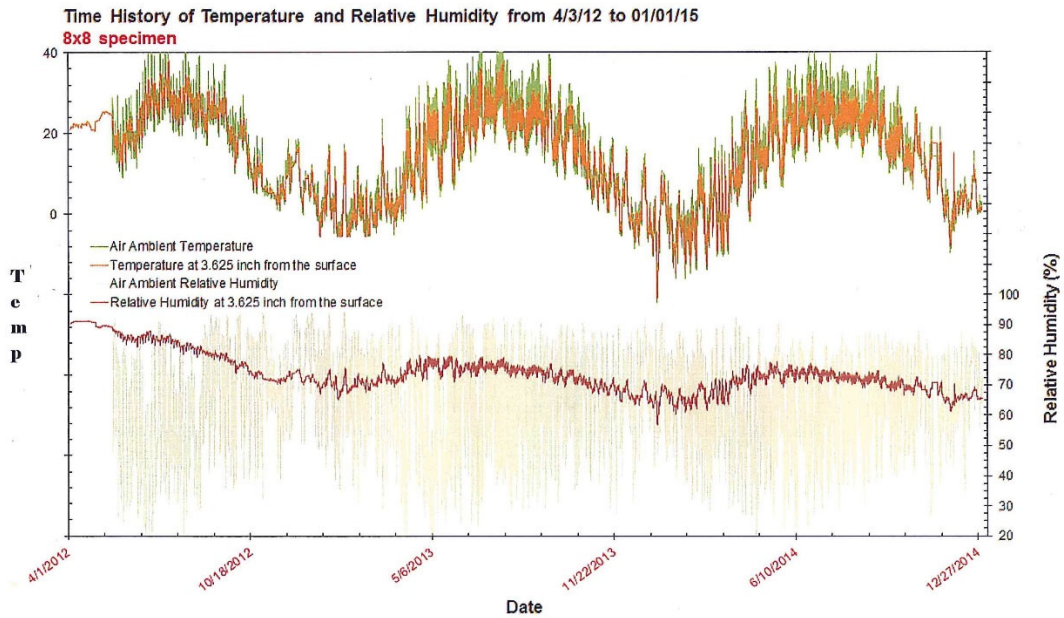


Figure 54. Time histories of RH for two years and eight months.

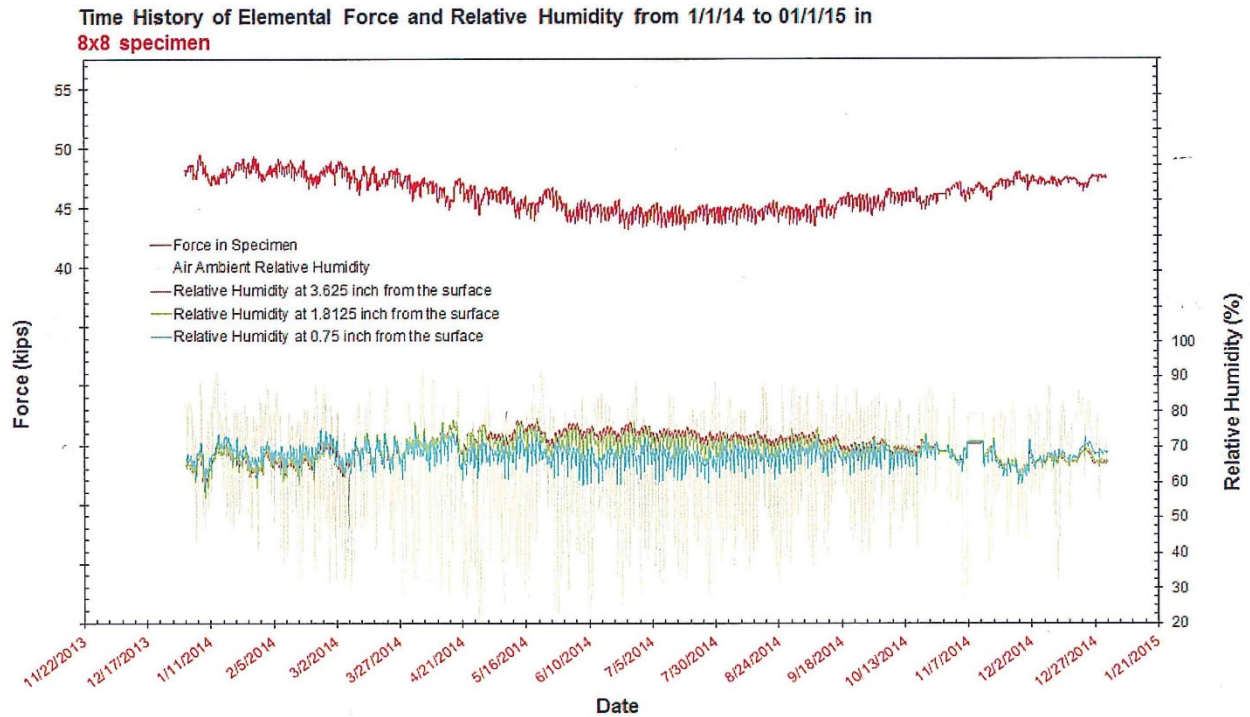


Figure 55. Time histories of RH over a period of approximately one year.

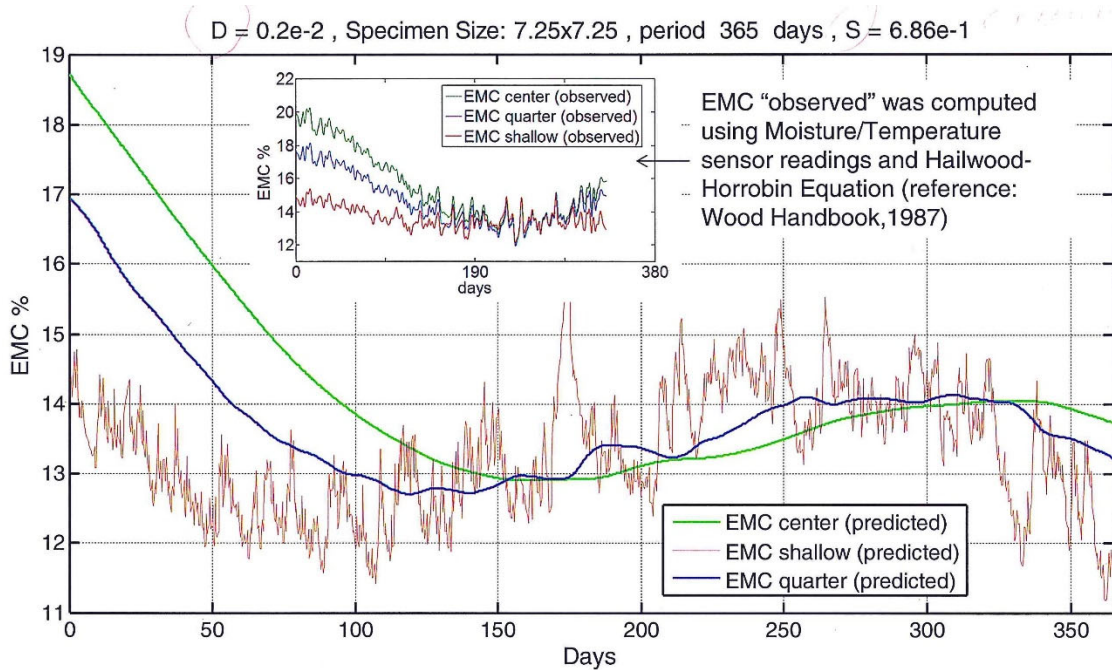


Figure 56. Time histories of equilibrium moisture contents.

The recorded temperature and RH values at three positions within the 8" x 8" were used in Equation 4-5 of the *Wood Handbook* to compute corresponding equilibrium moisture contents (EMCs) as a function of time. The resultant time histories of EMC are shown in the smaller figure inserted in Figure 56. The diffusion equation was then solved to try to analytically predict the observed evolution of moisture content (MC) within the section. The $C_e(t)$ function was computed from the recorded atmospheric temperature and RH time histories using Equation 4-5 of the *Wood Handbook*. The diffusion coefficient, D , and the surface emission coefficient, S , were adjusted to improve the match with the observed results. The analytically predicted moisture contents using $D = 0.2 \times 10^{-2} \text{ in}^2/\text{hour}$ and $S = 0.0068 \text{ in}/\text{hour}$ are shown in Figure 56. The computed results are a reasonable approximation of the observed results, although the analytically predicted MC near the surface of the 8" x 8" has higher frequency variations that do not appear in the observed values.⁵³

Although the 8" x 8" member was not re-tightened over the five years of study, the linear viscoelastic analysis formulation implemented in MATLAB was modified to study how re-tightening would affect the time-dependent strains and forces. As an initial study, a re-tightening action was applied after 100 days, after practically all the viscous losses from the initial post-tensioning force had occurred. Figure 57 shows time histories of viscous strains for five different values of the elastic modulus of wood. Figure 58 shows corresponding time histories of member axial force.

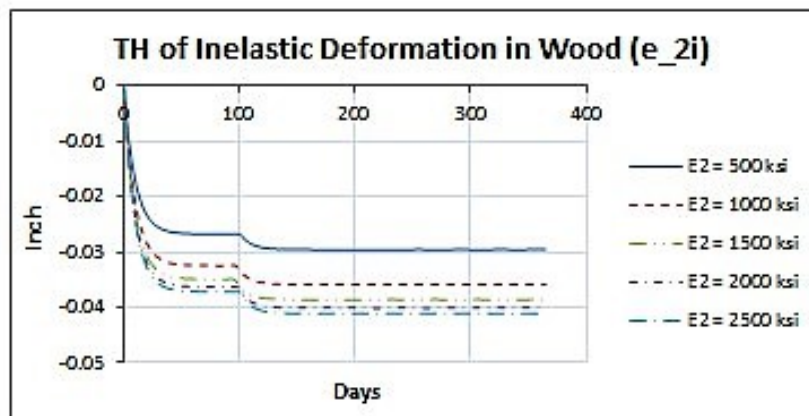


Figure 57. Time histories of viscous strain when re-tightening is done at 100 days.

⁵³ *Wood Handbook*, 4-3.

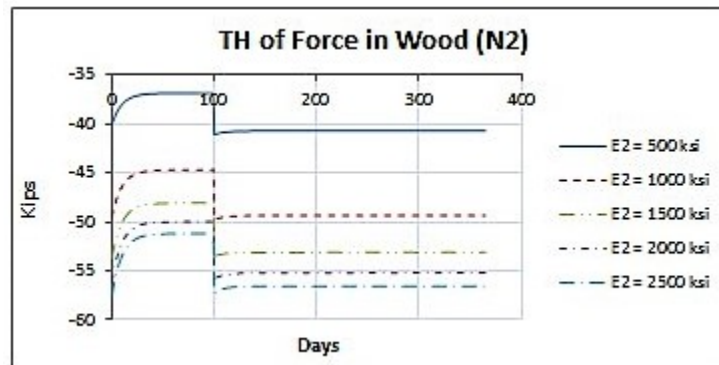


Figure 58. Time histories of member force when re-tightening is done at 100 days.

The first post-tensioning actions produced forces varying from -40 kips to -58 kips. The second post-tensioning actions, after 100 days of viscous losses, were designed to restore the member forces to values close to the original values. For example, for the case when the elastic modulus of wood equaled 1000 ksi, the initial force was -50 kips. The viscous losses decreased the force to -45 kips, and the second action restored the axial force to -50 kips. Some additional viscosity reduced the force to -49 kips. An important aspect of the predicted linear viscoelastic behavior is that the initial rate of viscous strain after a post-tensioning action is proportional to the change in the member force. That is, the viscous strain rate immediately after the initial post-tensioning is proportional to 50 kips, whereas the viscous strain rate after the re-tightening is proportional to the change in force, 50 kips – 45 kips = 5 kips. Therefore, the viscous strain rate after the re-tightening is much smaller and will cause smaller additional losses in force. In effect, re-tightening will produce a permanent increase in the member force.

Moose Brook West truss

Table 2 lists the significant events relative to the two post-tensioned trusses.

Date	Event
8/5/2011	Assembly of East truss in laboratory (no repaired nodes but one had an undetected crack)
3/16/2012	Assembly of West truss in laboratory (with repaired (brazed) nodes)
6/13/ 2012	Post-tensioning of West truss
6/14/2012	Post-tensioning of East truss
8/30/2012 to 9/11/2012	Leak in steam return line that caused high temperature and RH in laboratory
9/25/2012	Moving and installation of trusses outdoors
10/26/2012	Start of over six days of heavy rain from hurricane Sandy
8/20/2013	Re-tightening of West truss
9/16/2014	Removal of cover over trusses
10/27/2014	End of data acquisition and disassembly of trusses

Table 2. Timeline of significant events relative to the two post-tensioned trusses.

A total of eighteen strain gauges, nine per truss, were installed on the post-tensioning bars to control the prestress state; Figure 13 indicates the numbering of the bars. One Sensirion SHT 25 sensor was deployed to measure atmospheric temperature and RH. Fourteen Sensirion sensors were placed in the wood members; the installation was completed on January 11, 2013. Figure 59 shows time histories of the axial forces in the nine bars of the West truss, and a time history of the atmospheric RH. The time histories represent approximately two years and four months of data. As for the post-tensioned 8" x 8", the bar forces also show seasonal force variations of approximately 8 percent. Practically all the viscous losses occurred within the first four months. These losses were larger than in the 8" x 8", but they may be decreased considerably by using nodes with sleeves.⁵⁴ Re-tightening on August 20, 2013, increased the middle bar forces by about 30-35 kips; these changes in bar forces caused some additional viscous losses to force levels that were sustained for over a year. Slight increases in forces may be observed after the trusses were uncovered on September 16, 2014, and during the steam-return-line leak in the laboratory beginning on August 30, 2012. The latter time period is shown in two progressively finer time scales on Figures 60 and 61.

⁵⁴ Gasparini, Bruckner, and daPorto, "Time-Dependent Behavior."

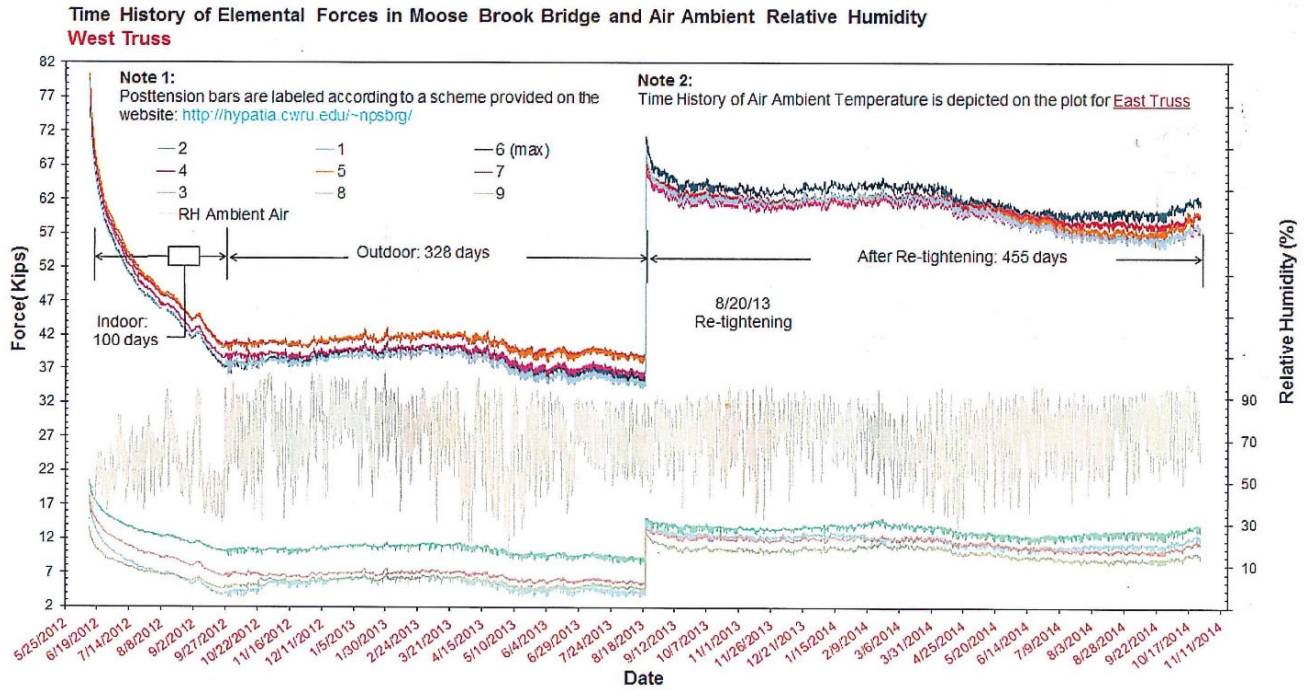


Figure 59. Time histories of member forces and atmospheric RH.

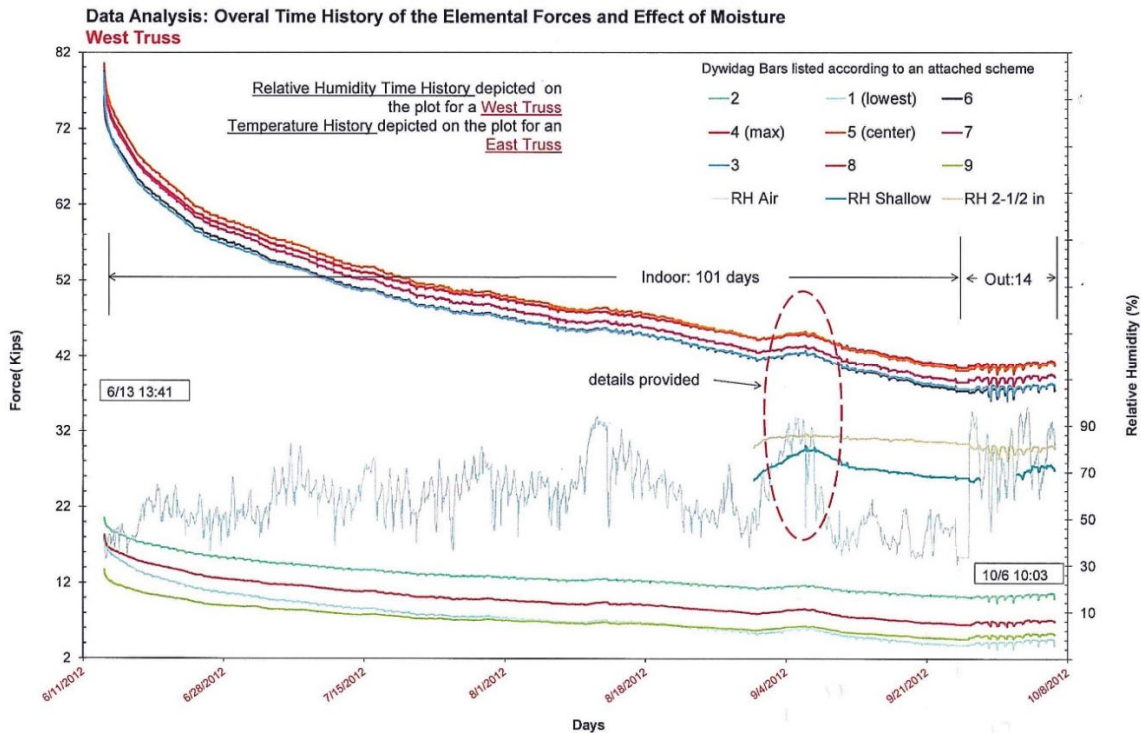


Figure 60. Time histories near the occurrence of a steam-return-line leak in the laboratory.

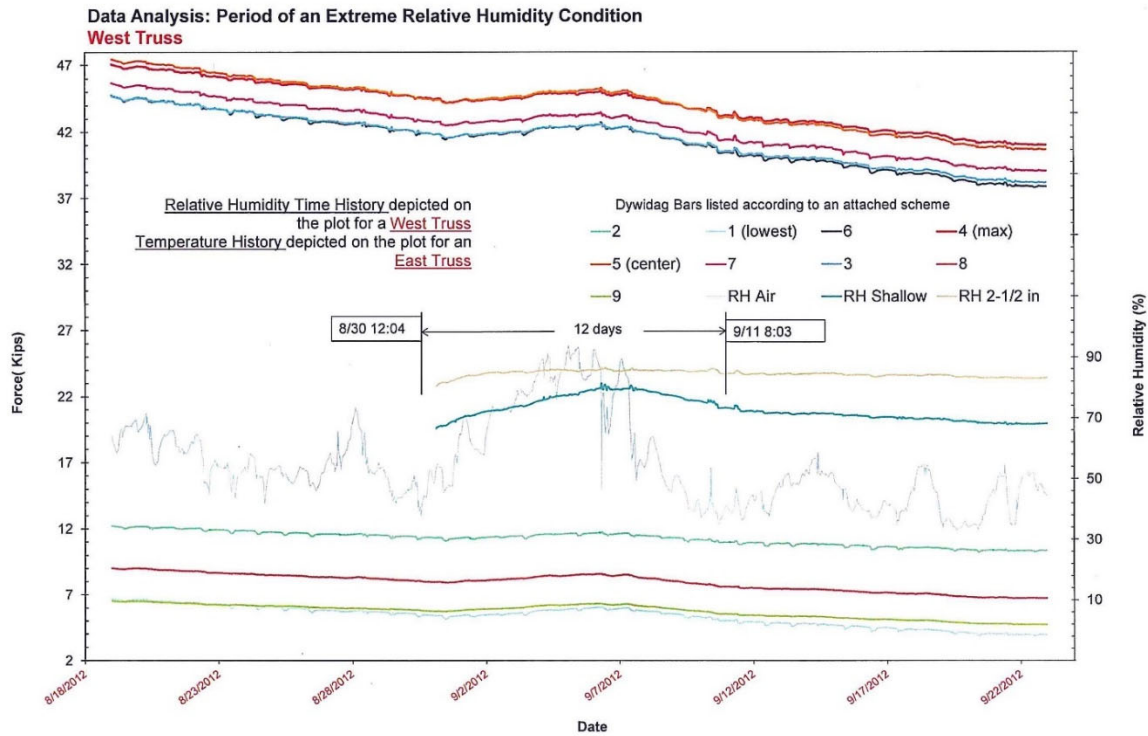


Figure 61. Time histories near the occurrence of a steam return line leak.

Figure 61 shows that the ten-day event of very high laboratory RH caused a slight increase in the wood RH near a member’s surface but almost no change in the sensor installed at a depth of 2-½. There was a slight increase in member axial forces.

Moose Brook East truss

As noted, the East truss was post-tensioned to forces approximately half those of the West truss because of a cracked and repaired cast-iron node at midspan. Figure 62 shows time histories of nine bar forces and the time history of the atmospheric temperature. Again, as noted for the 8" x 8", the member forces are inversely correlated with atmospheric temperatures. There are again small increases in bar forces during the steam return line leak and after removing the cover. Most of the prestress losses occurred during the first few months and the prestress forces appear permanent.

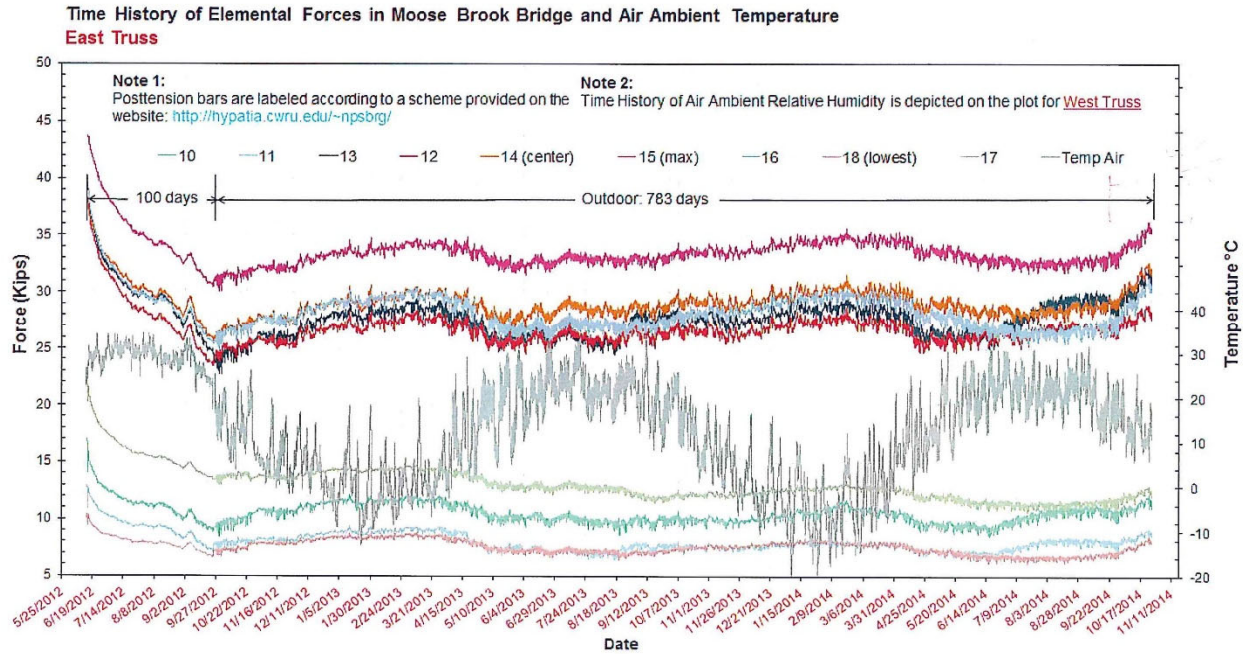


Figure 62. Time histories of bar forces and atmospheric temperature for the East truss.

One of the large diagonals (member 19) in the end panels was also instrumented with three Sensirion SHT 25 sensors at three depths. Figure 63 provides time histories of RH, and Figure 64 provides time histories of temperature in the member.

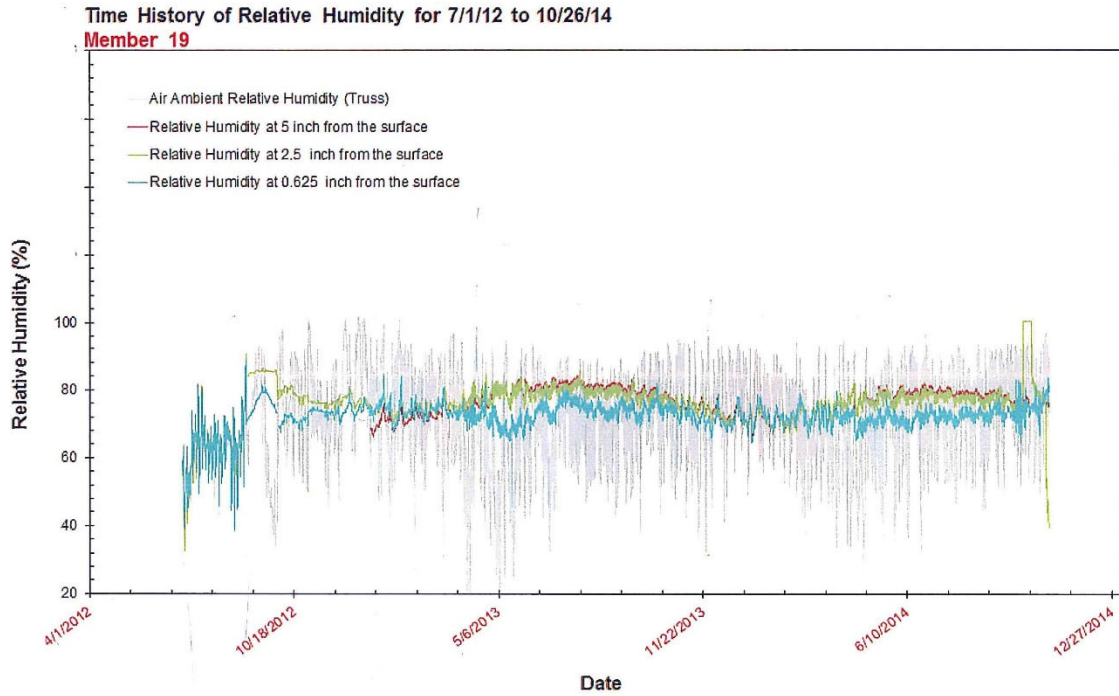


Figure 63. Time histories of wood RH at various depths.

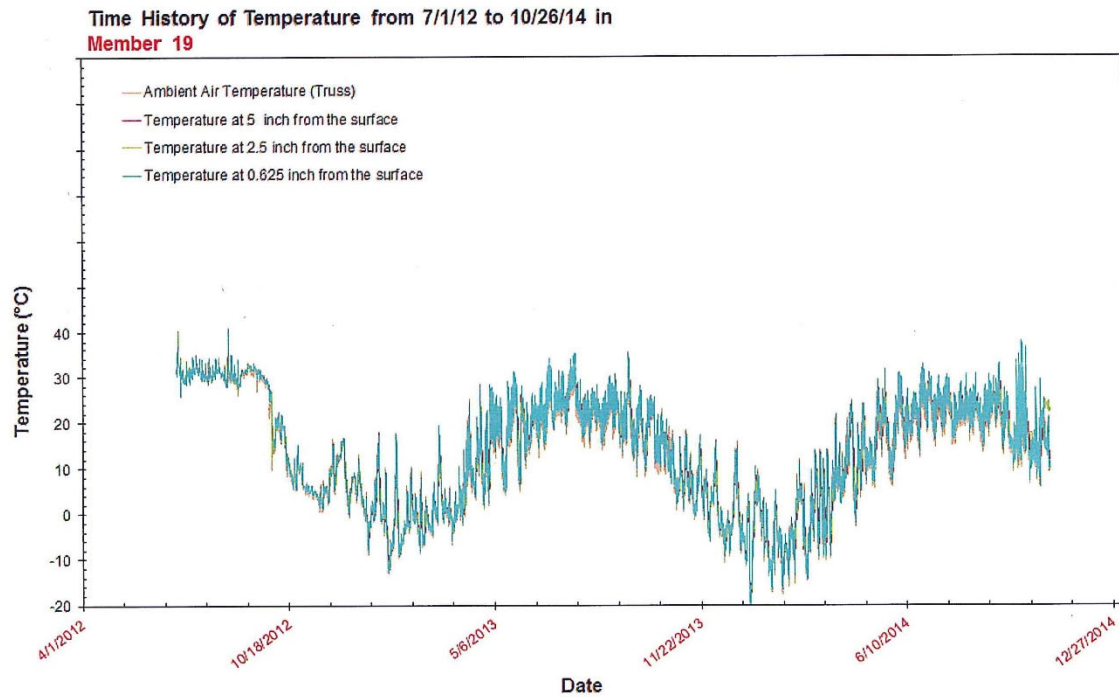


Figure 64. Time histories of wood temperature at various depths.

As observed for the 8" x 8" system, the RH is initially slightly higher at mid-depth (5" from the surface) than near the surface but the difference decreases in the winter months. The range in interior RH is much smaller than the range in atmospheric RH. Figure 64 shows that, at least at the large scale shown, temperatures within a member basically follow atmospheric temperatures. Although at a finer scale, there will be some differences in the range of temperature and some temporal lags as shown for the 8" x 8" in Figure 51.

ENGINEERING DESIGN AND ERECTION OF CLASSIC POST-TENSIONED HOWE TRUSS BRIDGES

Thousands of classic, statically indeterminate, post-tensioned, wooden Howe truss bridges were built in the U.S. from the 1840s into the twentieth century. Most were for very demanding railroad loads. They were cost-effective and extremely reliable systems. This constitutes a remarkable American engineering heritage that should be understood, valued, and continued.

The primary observations from the completed research are:

- There will be viscous losses after post-tensioning a wooden Howe truss, primarily in the first few months, but a permanent prestress state can be achieved.
- There will be force fluctuations in the members from daily and seasonal atmospheric temperature fluctuations. For the trusses instrumented in Cleveland, Ohio, the range in the seasonal fluctuations was approximately 8 percent.
- The hygroscopicity of wood and atmospheric RH changes have small effects on member axial forces. Observed “mechanosorptive” effects on axial forces were also small.

Linear elastic modeling may be used for the design of post-tensioned wooden Howe trusses, considering the post-tensioning action, dead load, live load, and wind. Analysis models must recognize that a classic Howe truss has tension-only and compression-only members. There will be prestress losses from wood viscosity but they may be minimized by these conceptual design features:

- Use small diameter (small axial stiffness), high-strength prestressing bars.
- Use fabricated steel nodes with sleeves to prevent normal stresses perpendicular to the grain of the chords.
- Prestress the truss in warm weather.

If it is necessary to estimate the mechanism limit state capacity of a Howe truss, an incremental load sequence may be used, keeping in mind that there are tension-only and compression-only members. It is important to understand that, **if the members have ductile strengths, the mechanism limit state capacity of a Howe truss will not be decreased by the prestress forces.**

The post-tensioning process must be thoughtfully prescribed by the designer and controlled by load transducers, such as load cells. It should be noted that Howe trusses are stable, out-of-plane during and after post-tensioning. This was demonstrated when the two planar, post-tensioned, laterally unsupported Howe trusses were moved outdoors as shown in Fig. 34. Therefore, normal lateral wind bracing will be more than sufficient during post-tensioning.

FINAL REASSEMBLY OF TRUSSES

On October 27, 2014, the CWRU team disassembled two trusses and loaded the members on a flatbed truck for shipment back to Gorham, New Hampshire, as shown in Figure 65. The relative ease of assembly and disassembly is one of the significant features of Howe trusses. After negotiations with two prospective partners in New Hampshire fell through, NSPCB began discussions with the Wiscasset, Waterville & Farmington Railway Museum (WW&F) in Alna, Maine, in 2015. The WW&F saw the available bridge as an exciting opportunity to extend their 2.6-mile excursion line another 0.75 miles north over its historic right-of-way, across Trout Brook, to the Trout Brook Preserve wayside on Route 218. WW&F, NSPCB, and NPS signed a memorandum of agreement on October 9, 2017, for the Moose Brook Bridge to be donated, delivered, and re-erected at the museum. In exchange, the museum would be responsible for the engineering, site work, moving the bridge, right-of-way clearing, and laying of the track. WW&F Railway Superintendent and Chief Mechanical Officer Jason M. Lamontagne led the planning.⁵⁵

Meanwhile, Timothy Andrews began erecting the twin Howe trusses one last time at the museum's parking lot in November 2017, working with a volunteer WW&F crew to reassemble the bridge timbers and "tune" the trusses. Tuning involved tightening the verticals and adjusting the diagonals. In summer 2018, the team positioned the trusses vertically, Andrews installed floor beams and two outriggers with replicated rods. He then enclosed each truss by applying vertical white pine shiplap siding, and laid asphalt roll roofing atop a white pine roof deck, to match the original boxed pony. After spraying Nochar fire retardant onto the trusses and siding, the volunteers stained the sheathing red to match the Boston and Maine Railroad color scheme.

⁵⁵ "Narrow Bridge Ahead!" Wiscasset, Waterville & Farmington Railway Museum website, <http://wwfry.org/?p=1627>, last updated October 13, 2017.

On June 9, 2018, NSPCB president Bill Caswell officially transferred ownership of the bridge over to WW&F president David Buczkowski (Figures 66a-d).

In August 2018, Chesterfield Associates drove piles and attached pile caps at the bridge site. WW&F volunteers erected stone-filled timber cribs to support the short approach spans. On September 8, 2018, the WW&F crew transported the assembled bridge 3 miles and rolled it into position on the cribbed piers over Trout Brook (Figures 66e-f). Finally, they installed sleeper beams over the floor beams of the Howe truss span and the approach spans, and decked the bridge end-to-end with solid-sawn timber. As of March 2019, the WW&F has completed tree clearing to the bridge, and will repair the right-of-way in preparation for the final 2,000' of track construction. Steam excursion trains are expected to start running over the bridge in 2020. After a long journey beginning as charred remains in 2009 over Moose Brook in Gorham, New Hampshire, the reconstructed Howe pony truss had finally found a permanent home over Trout Brook on the Wiscasset, Waterville & Farmington Railway in Alna, Maine.



Figure 65. Howe trusses disassembled and ready for shipment back to Gorham, New Hampshire, October 2014.

BOSTON & MAINE RAILROAD, BERLIN BRANCH BRIDGE #148.81
(Moose Brook Bridge)
HAER No. NH-48
(Page 69)



Figure 66a-b. Reassembled Howe trusses with outriggers. Timothy Andrews sprayed NoChar fire retardant on all truss members and planks of siding, May 2018.



Figure 66c-d. With the trusses fully sheathed, NSPCB President Bill Caswell signed over transfer of the bridge to WW&F President David Buczkowski on June 9, 2018. Next, the bridge was painted B&M red.



Figure 66e-f. WW&F volunteers moved the bridge three miles and placed it atop cribbed piers over Trout Brook in September 2018. WW&F photos.



Figure 67. Completed Moose Brook Bridge over Trout Brook in Alna, Maine, on the future WW&F excursion line, December 2018. WW&F photo.

SOURCES OF INFORMATION

Allen, Richard Sanders. *Covered Bridges of the Middle Atlantic States*. Brattleboro, VT: Stephen Greene Press, 1959.

_____. *Covered Bridges of the Northeast*. Brattleboro, VT: Stephen Greene Press, 1957.

Anderson, Richard K. and Emory L. Kemp. "Reading-Halls Station Bridge." HAER No. PA-55, Historic American Engineering Record (HAER), National Park Service, U.S. Department of the Interior, 1987.

Andrews, Timothy. Email to Christopher Marston, November 30, 2011.

Baronas, R., F. Ivanauskas, I. Juodeikienė, and A. Kajalavičius. "Modeling of Moisture Movement in Wood during Outdoor Storage." *Nonlinear Analysis: Modeling and Control* 6, no. 2 (2001): 3-14.

Boston & Maine Railroad Engineering Department. "Bridge List—New Hampshire Division," 1945.

"Bridge Superstructure." *Transactions of the American Society of Civil Engineers* (1878): 340.

Brischke, C., A. O. Rapp, and R. Bayerbach. "Measurement system for long-term recording of wood moisture content with internal conductively glued electrodes." *Building and Environment* 43, no. 10 (2008): 1566-1574.

Caswell, C. E. *Boston, Concord & Montreal: Story of the Building and Early Days of This Road*. Warren, NH: The News Press, 1919.

Choong, E. T. and C. Skaar. "Separating internal and external resistance to moisture removal in wood drying." *Wood Science* 1 (1969): 200-202.

Christianson, Justine and Christopher H. Marston, executive editors. *Covered Bridges and the Birth of American Engineering*. Washington, DC: Historic American Engineering Record, National Park Service, 2015.

Concord & Montreal Railroad. *Report of the Directors to the Stockholders*, 1918.

Conwill, Joseph D. "Pony Trusses for the Iron Horse." *Covered Bridge Topics*, Summer 1993, 14.

_____. "Wright's Bridge." HAER No. NH-35, *Historic American Engineering Record* (HAER), National Park Service, U.S. Department of the Interior, 2002.

Cooper, Theodore. "American Railroad Bridges." *Transactions of the American Society of Civil Engineers* 21 (July 1889): 1-58.

Cutter, Louis F. "Appalachian Mountain Club Map of the Northern Peaks of the Great Range White Mountains, N.H." 1914.

Crank, J. *The Mathematics of Diffusion*. 2nd ed. Oxford: Clarendon Press, 1975.

Fletcher, Robert and J.P. Snow. "A History of the Development of Wooden Bridges." *Proceedings of the American Society of Civil Engineers* (November 1932): 314-354.

Fotsing, Joseph A.M. and Claude W. Tchagang. "Experimental determination of the diffusion coefficients of wood in isothermal conditions." *Heat Mass Transfer* 41 (September 2005): 977-980.

Fridley, K. J. "Designing for creep in wood structures." *Forest Products Journal* 42, no. 3 (1992): 23-28.

Garvin, James L. "Chronology of Planning and Work: Boxed Railroad Pony Truss Bridge, Gorham, New Hampshire." Concord: New Hampshire Division of Historical Resources, 2009.

_____. "Sketch of Moose Brook Bridge." Unpublished drawing. May 1980.

Gasparini, D.A., J. Bruckner, and F. da Porto. "Time-Dependent Behavior of Posttensioned Wood Howe Bridges." *ASCE Journal of Structural Engineering* 132, no. 3 (March 2006): 418-29.

Gasparini, D.A. "Whistler, Howe, and Stone: The Design and Construction of the Western Railroad's Bridge over the Connecticut River 1840-1841." *Proceedings of the Fifth International Congress on Construction History*, Chicago, IL (June 3-7, 2015): 161-168.

Gasparini, D.A., K. Nizamiev, and C. Tardini. "G.W. Whistler and the Howe Bridges on the Nikolaev Railway, 1842-1851." *ASCE Journal of Performance of Constructed Facilities* 30, no. 3 (June 2016): 1-16.

Hailwood, A. J. and S. Horrobin. "Absorption of water by polymers: Analysis in terms of a simple model." *Transactions of the Faraday Society* 42 (1946): 84-102.

Heald, Bruce D. *A History of the Boston & Maine Railroad: Exploring New Hampshire's Rugged Heart by Rail*. Charleston, SC: The History Press, 2007.

Historic American Engineering Record (HAER). National Park Service, U.S. Department of the Interior, "Clark's Bridge," HAER NH-39.

_____. "Philadelphia, Wilmington & Baltimore Railroad, President Street Station," HAER No. MD-8.

_____. "Junction Road Bridge," HAER No. OH-97.

_____. "Snyder Brook Bridge," HAER No. NH-49.

_____. "Station Road Bridge," HAER No. OH-67.

_____. "Wheeling Suspension Bridge," HAER WV-2.

_____. "Wright's Bridge," HAER No. NH-35.

Holzer, Stefan M. *Die König-Ludwig-Brücke Kempten*. Historische Wahrzeichen Ingenieurbaukunst in Deutschland, Band 11. Berlin: Bundesingenieurkammer, 2012.

Houška, M. and Pino Koc. "Sorptive Stress Estimation: An Important Key to the Mechano-Sorptive Effect in Wood." *Mechanics of Time-Dependent Materials* 4 (March 2000): 81-98.

"Howe, William." *National Cyclopaedia of American Biography* VII (1897): 507.

Howe, William. U.S. Letters Patent No. 1,711, 3 August 1840.

- Hunt, David G. and Christopher F. Shelton. "Progress in the analysis of creep in wood during concurrent moisture changes." *Journal of Materials Science* 22, no. 1 (1987): 313-320.
- Husson, J. M., F. Dubois, and N. Sauvat. "Elastic response in wood under moisture content variations: analytic development." *Mechanics of Time-Dependent Materials* 14, no. 2 (2010): 203-217.
- Lawry, Nelson H. "Boston & Maine's Boxed Ponies: Galloping Into Oblivion?" *Trains*, February 1994, 44-47.
- _____. "Boston & Maine's Boxed Ponies: Losing the Race." *Railpace*, April 1998: 39.
- _____. E-mail correspondence with Lola Bennett, July 13 and July 16, 2009.
- Lindsell, Robert M. *The Rail Lines of Northern New England: A Handbook of Railroad History*. Pepperell, MA: Branch Line Press, 2000.
- Leicester, R. H. "A Rheological Model for Mechano-sorptive Deflections of Beams." *Wood Science and Technology* 5 (1971): 211-220.
- Mårtensson, A. "Mechano-sorptive effects in wooden material." *Wood Science and Technology* 28, no. 6 (1994): 437-449.
- Martin, Charles F. *New Hampshire Rail Trails*. Pepperell, MA: Branch Line Press, 2008.
- Miller, Terry. "Ohio Rail Covered Bridges." Unpublished manuscript, 1967.
- "Narrow Bridge Ahead!" Wiscasset, Waterville & Farmington Railway Museum website, <http://wwfry.org/?p=1627>, last updated October 13, 2017.
- "New Hampshire's Presidential Rail Trail." <https://www.railstotrails.org/trailblog/2014/december/09/new-hampshire-s-presidential-range-rail-trail/>, last updated December 9, 2014.
- Newman, A. B. "The Drying of Porous Solids: Diffusion and Surface Emission Equations." *Transactions of the American Institute of Chemical Engineers* 27 (1931): 203-211.

- _____. "The Drying of Porous Solids: Diffusion Calculations." *Transactions of the American Institute of Chemical Engineers* 27 (1931): 310-333.
- Robitaille, Paul. "Gorham's Pony Truss Bridge: Hopes Are That It Can Be Rebuilt." *The Berlin Reporter*, September 29, 2004, A3.
- Rosen, Howard N. "The Influence of External Resistance on Moisture Adsorption Rates in Wood." *Wood and Fiber Science* 10, no. 3 (Fall 1978): 218-228.
- Simpson, William T. "Predicting Equilibrium Moisture Content of Wood by Mathematical Models." *Wood and Fiber* 5, no. 1 (Spring 1973): 41-49.
- _____. "Equilibrium Moisture Content of Wood in Outdoor Locations in the United States and Worldwide." Research Note FPL-RN-0268. Madison, WI: U.S. Department of Agriculture, Forest Service, Forest Products Laboratory, 1998.
- Simpson, W. T. and J. Y. Liu. "An Optimization Technique to Determine Red Oak Surface and Internal Moisture Transfer Coefficients During Drying." *Wood and Fiber Science* 29, no. 4 (October 1997): 312-318.
- Skaar, C. "Analysis of Methods for Determining the Coefficient of Moisture Diffusion in Wood." *Journal of Forest Products Research Society* 4, no. 6 (1954): 403-410.
- Snow, J. Parker. "Wooden Bridge Construction on the Boston & Maine Railroad." *Journal of the Association of Engineering Societies* 15 (July 1895): 31-43.
- Wood Handbook: Wood as an Engineering Material*. General Technical Report FPL-GTR-190. Madison, WI: U.S. Department of Agriculture, Forest Service, Forest Products Laboratory, 2010.
- Wright, David W., editor. *World Guide to Covered Bridges*. 7th edition. Concord, NH: The National Society for the Preservation of Covered Bridges, 2009.